INTERNATIONAL JOURNAL OF
NUMERICAL ANALYSIS AND MODELING
Volume 17, Number 1, Pages 118–150

3D B_2 MODEL FOR RADIATIVE TRANSFER EQUATION

RUO LI AND WEIMING LI

Abstract. We proposed a 3D B_2 model for the radiative transfer equation. The model is an extension of the 1D B_2 model for the slab geometry. The 1D B_2 model is an approximation to the 2nd order maximum entropy (M_2) closure and has been proved to be globally hyperbolic. In 3D space, we are basically following the method for the slab geometry case to approximate the M_2 closure by B_2 ansatz. Same as the M_2 closure, the ansatz of the new 3D B_2 model has the capacity to capture both isotropic solutions and strongly peaked solutions. And beyond the M_2 closure, the new model has fluxes in closed-form such that it is applicable to practical numerical simulations. The rotational invariance, realizability, and hyperbolicity of the new model are carefully studied.

Key words. Radiative transfer, moment model, maximum entropy closure.

1. Introduction

The radiative transfer equations describe the transportation of photons in a medium [22, 20]. They are *kinetic equations*, and the unknown is the specific intensity of photons. The specific intensity is a function of time, spatial coordinates, frequency, and angular variables. There are numerous methods for solving the radiative transfer equations [12, 5, 26, 8, 19]. The moment method is an efficient approach for reducing the computation cost brought about by the high-dimensionality of variables of kinetic equations.

In most applications, the quantities of interest are the few lowest order moments. Therefore moments are proper choices for discretizing the angular variables. In fact, in many applications, people are only concerned with the zeroth order moment and a diffusion equation is often solved to approximate the radiation process [29]. However, the diffusion equation might not be a very accurate approximation when the radiation field is away from equilibrium, therefore more moments are sometimes needed. An essential problem in the moment method is that moment systems are not closed. Closing the system by specifying a constitutive relationship is known as the *moment-closure problem*. One approach towards moment-closure is to recover the angular dependence of the specific intensity from the known moments. The reconstructed specific intensity is called an *ansatz*. Ideally, the ansatz should be non-negative for all moments which can be generated by a non-negative distribution. Also, one would like the system to be hyperbolic since hyperbolicity is necessary for the local well-posedness of Cauchy problem. Other natural requirements include that the ansatz satisfies rotational invariance and reproduces the isotropic distribution at equilibrium. Numerous forms of ansätze have been studied in the literature. For detailed descriptions of standard methods we refer to [22, 18]. Yet, in multi-dimensional cases, the maximum entropy method, referred to as the M_n model, is perhaps the only method known so far to have both

Received by the editors June 6, 2019.
2000 *Mathematics Subject Classification.* 35Q35, 82C70.

realizability and global hyperbolicity [7]. However, the flux functions of the maximum entropy method are generally not explicit [1], so numerically computing such models involve solving highly nonlinear and probably ill-conditioned optimization problems frequently. There have been continuous efforts on speeding up the computation process [2, 1, 10]. Recently, there are also attempts in deriving closed-form approximations of the maximum entropy closure in order to avoid the expensive computations. For 1D cases, an approximation to the M_n models using the Kershaw closure is given in [23]. For multi-dimensional cases, a model based on directly approximating the closure relations of the M_1 and M_2 methods is proposed in [21]. Our work in this paper also aims at constructing closed-form approximations of the maximum entropy model. Like [21], we seek a closed-form approximation to the M_2 method in 3D. But unlike [21], we derive our model from an ansatz with some similarity to that of the M_2 model.

In a previous study [3], we analyzed the second order extended quadrature method of moments (EQMOM) introduced in [27] which we call the B_2 model. In this work, we propose an approximation of the M_2 model in 3D space by extending the B_2 model studied in [3] to 3D. The reason for this approach is that the B_2 ansatz shares the following properties with the M_2 ansatz:

(1) it interpolates smoothly between isotropic and strongly peaked distribution functions;
(2) it captures anisotropy in opposite directions.

The B_2 closure in [3] is for slab geometries. Preserving rotational invariance when extending it to 3D space is non-trivial. We use the sum of the axisymmetric B_2 ansätze in three mutually orthogonal directions as the ansatz for a second order moment model in 3D space. This new model is referred to as the *3D B_2 model*. The consistency of known moments requires the three mutually orthogonal directions to be the three eigenvectors of the second-order moment matrix. We point out that there are three free parameters in the ansatz of the 3D B_2 model after the consistency of known moments is fulfilled. These parameters are specified as functions of the first-order moments and the eigenvalues of the second-order moment matrix. We prove that the 3D B_2 model is rotationally invariant. The region where the model possesses a non-negative ansatz is illustrated, as well as the hyperbolicity region of the model with vanished first-order moment. Though far from perfect, the 3D B_2 model shares some important features of the M_2 closure. Also, the model has explicit flux functions, making it very convenient for numerical simulations.

The rest of this paper is organized as follows. In Section 2 we recall the basics of moment models, and briefly, introduce the M_2 method as well as the B_2 model for 1D slab geometry. In Section 3 we propose the 3D B_2 model. In Section 4 we analyze its properties. Finally, in Section 5 we summarize and discuss future work.

2. Preliminaries

The specific intensity $I(t, \mathbf{r}, \nu, \mathbf{\Omega})$ is governed by the radiative transfer equation

$$\frac{1}{c}\frac{\partial I}{\partial t} + \mathbf{\Omega}\cdot\nabla I = \mathcal{C}(I), \tag{1}$$

where c is the speed of light. The variables in the equation are time $t \in \mathbb{R}^+$, the spatial coordinates $\mathbf{r} = (x, y, z) \in \mathbb{R}^3$, the angular variables $\mathbf{\Omega} = (\Omega_x, \Omega_y, \Omega_z) \in \mathbb{S}^2$, and frequency $\nu \in \mathbb{R}^+$. The right-hand side $\mathcal{C}(I)$ describes the interactions between

[1] With the first order maximum entropy model for the grey equations as the only exception [7].

photons and the background medium and are not the focus of this paper. A typical right-hand side takes the form

$$\mathcal{C}(I) = -\sigma_a I(\mathbf{\Omega}) - \sigma_s \left(I(\mathbf{\Omega}) - \frac{1}{4\pi} \int_{\mathbb{S}^2} I(\mathbf{\Omega}) \, \mathrm{d}\mathbf{\Omega} \right), \tag{2}$$

where σ_a and σ_s are constant parameters. We introduce the moment method in the context of second order models. Let

$$\begin{aligned} \mathbf{v} = [\quad & 1, \\ & (\mathbf{\Omega}\cdot\mathbf{e}_x), \quad (\mathbf{\Omega}\cdot\mathbf{e}_y), \quad (\mathbf{\Omega}\cdot\mathbf{e}_z), \\ & (\mathbf{\Omega}\cdot\mathbf{e}_x)^2, \quad (\mathbf{\Omega}\cdot\mathbf{e}_x)(\mathbf{\Omega}\cdot\mathbf{e}_y), \quad (\mathbf{\Omega}\cdot\mathbf{e}_x)(\mathbf{\Omega}\cdot\mathbf{e}_z), \\ & \qquad (\mathbf{\Omega}\cdot\mathbf{e}_y)^2, \quad (\mathbf{\Omega}\cdot\mathbf{e}_y)(\mathbf{\Omega}\cdot\mathbf{e}_z) \quad]^T. \end{aligned} \tag{3}$$

Use $\mathbf{e}_x$, $\mathbf{e}_y$ and $\mathbf{e}_z$ to denote the unit vectors along the coordinate axes. Define

$$\langle \psi \rangle := \int_{\mathbb{S}^2} \psi(\nu, \mathbf{\Omega}) \, \mathrm{d}\mathbf{\Omega}.$$

Multiplying equation (1) by the vector $\mathbf{v}$ defined in (3) and integrating over the angular variables give

$$\frac{1}{c}\frac{\partial \langle \mathbf{v} I \rangle}{\partial t} + \frac{\partial \langle \Omega_x \mathbf{v} I \rangle}{\partial x} + \frac{\partial \langle \Omega_y \mathbf{v} I \rangle}{\partial y} + \frac{\partial \langle \Omega_z \mathbf{v} I \rangle}{\partial z} = \langle \mathbf{v} \mathcal{C}(I) \rangle . \tag{4}$$

In system (4), the time evolution of second-order moments relies on third-order moments. Therefore (4) is not a closed system. If we approximate the third-order moments in (4) using lower order moments, we could get a closed system. Let[2]

$$E^0 \simeq \langle I \rangle, \quad \mathbf{E}^1 \simeq \langle \mathbf{\Omega} I \rangle, \quad \mathbf{E}^2 \simeq \langle \mathbf{\Omega} \otimes \mathbf{\Omega} I \rangle, \quad \mathbf{E}^3 \simeq \langle \mathbf{\Omega} \otimes \mathbf{\Omega} \otimes \mathbf{\Omega} I \rangle .$$

A closed system of equations has the form

$$\begin{aligned} &\frac{1}{c}\frac{\partial E^0}{\partial t} + \nabla\cdot\mathbf{E}^1 = r^0(E^0, \mathbf{E}^1, \mathbf{E}^2), \\ &\frac{1}{c}\frac{\partial \mathbf{E}^1}{\partial t} + \nabla\cdot\mathbf{E}^2 = \mathbf{r}^1(E^0, \mathbf{E}^1, \mathbf{E}^2), \\ &\frac{1}{c}\frac{\partial \mathbf{E}^2}{\partial t} + \nabla\cdot\left[\mathbf{E}^3(E^0, \mathbf{E}^1, \mathbf{E}^2)\right] = \boldsymbol{r}^2(E^0, \mathbf{E}^1, \mathbf{E}^2). \end{aligned} \tag{5}$$

The choice of $\mathbf{E}^3$, r^0, $\mathbf{r}^1$, and $\boldsymbol{r}^2$ specify a *closure*. The system (5) is a second order moment model. The following properties of a moment model concern us the most, which were frequently discussed in the literature.

Rotational invariance: We use the definition of rotational invariance as in [15]. Consider a moment system in multi-dimensions,

$$\frac{\partial \mathbf{U}}{\partial t} + \sum_{i=1}^{D} \frac{\partial \mathbf{F}_i(\mathbf{U})}{\partial x_i} = \boldsymbol{\mathcal{C}}(\mathbf{U}). \tag{6}$$

For fixed rotation matrix $\mathbf{T} \in SO(D)$, denote Γ as the rotation transformation which associates physical quantities in coordinate system $\mathbf{x}$ to the rotated system $\tilde{\mathbf{x}} = \mathbf{T}\mathbf{x}$. The moment system satisfies rotational invariance if for any rotation transformation Γ we have the following relationship

$$\frac{\partial \Gamma \mathbf{U}}{\partial t} + \sum_{k=1}^{D} \frac{\partial \mathbf{F}_i(\Gamma \mathbf{U})}{\partial \tilde{x}_k} = \boldsymbol{\mathcal{C}}(\Gamma \mathbf{U}).$$

[2]The notation $a \simeq b$ means 'a is an approximation of b.'

Hyperbolicity: Let $\mathbf{J}_i$ be the Jacobian matrix of the flux function $\mathbf{F}_i$ in equation (6). The system (6) is hyperbolic if for any unit vector $\mathbf{n} \in \mathbb{R}^D$, $\sum_{i=1}^{D} n_i \mathbf{J}_i$ is real diagonalizable.

Realizability: The realizability domain is defined as moments which could be generated by a nonnegative distribution function [14]. More precisely, the realizable moments which this paper is concerned with are those generated by functions in

$$D := \{f \geq 0 : f \in L^1(\mathbb{S}^2), f \not\equiv 0\}^3.$$

A closure is said to be realizable if the higher order moments it closes belong to the realizability domain.

For one dimensional problems, [6] gives necessary and sufficient conditions for realizability. Its results cover moments of arbitrary order. For multi-dimensional cases, only the conditions for the first and second order models are currently known [16], while the conditions for moments of higher order remain open problems.

The maximum entropy models are equipped with all the properties mentioned above. For detailed discussions we refer to [14, 17, 7]. We review the principles for deriving the maximum entropy models by taking the second order case as an example. It is called the M_2 model. Solve the following constrained variational minimization problem

$$\begin{aligned} &\text{minimize } H(I) \\ &\text{subject to } \langle I \rangle = E^0, \langle \mathbf{\Omega} I \rangle = \mathbf{E}^1, \text{and } \langle \mathbf{\Omega} \otimes \mathbf{\Omega} I \rangle = \mathbf{E}^2 \end{aligned} \tag{7}$$

where $H(I)$ is the Bose-Einstein entropy

$$H(I) := \left\langle \frac{2k_B \nu^2}{c^3} \left(\chi I \log(\chi I) - (\chi I + 1) \log(\chi I + 1) \right) \right\rangle, \tag{8}$$

where $\chi = \dfrac{c^2}{2\hbar \nu^3}$. This gives us an ansatz

$$\hat{I}_M(\nu, \mathbf{\Omega}) = \frac{1}{\chi} \left(\exp\left(-\frac{\hbar \nu}{k_B} \boldsymbol{\alpha} \cdot \mathbf{v} \right) - 1 \right)^{-1}, \tag{9}$$

where $\boldsymbol{\alpha} \cdot \mathbf{v}$ is a second order polynomial of $\mathbf{\Omega} \in \mathbb{S}^2$. The parameters $\boldsymbol{\alpha}$ is the unique vector such that

$$\left\langle \hat{I}_M \right\rangle = E^0, \quad \left\langle \mathbf{\Omega} \hat{I}_M \right\rangle = \mathbf{E}^1, \text{and} \quad \left\langle \mathbf{\Omega} \otimes \mathbf{\Omega} \hat{I}_M \right\rangle = \mathbf{E}^2.$$

The M_2 method is defined by taking

$$\begin{aligned} &\mathbf{E}^3 := \left\langle \mathbf{\Omega} \otimes \mathbf{\Omega} \otimes \mathbf{\Omega} \hat{I}_M \right\rangle, \qquad && r^0 := \left\langle \mathcal{C}(\hat{I}_M) \right\rangle, \\ &\mathbf{r}^1 := \left\langle \mathbf{\Omega} \mathcal{C}(\hat{I}_M) \right\rangle, && \boldsymbol{r}^2 := \left\langle \mathbf{\Omega} \otimes \mathbf{\Omega} \mathcal{C}(\hat{I}_M) \right\rangle \end{aligned} \tag{10}$$

in (5).

However, the M_2 closure is not given explicitly, so (10) has to be computed by solving the optimization problem (7) numerically. The numerical optimization at each time step for all spatial grid is extremely expensive.

Recent work [21] proposes an approximation of the M_2 method in multi-dimensions by directly approximating its closure relation, though the ansatz corresponding to

---

[3] For more rigorous discussions on definitions of the moment problem we refer to [24].

the closure is not clarified. We adopt the approach of constructing an ansatz to approximate the M_2 ansatz, then the closure relation is given naturally as in (10).

In a previous work [3], we examined the properties of the second order extended quadrature method of moments (EQMOM) proposed in [27] in slab geometry, and the model was referred as the B_2 model. In EQMOM, the ansatz $\hat{I}$ is reconstructed by a combination of beta distributions. The beta distribution as a function of $\mu \in [-1,1]$ is given by

$$\mathcal{F}(\mu;\gamma,\delta) = \frac{1}{2\boldsymbol{B}(\xi,\eta)}\left(\frac{1+\mu}{2}\right)^{\xi-1}\left(\frac{1-\mu}{2}\right)^{\eta-1}, \quad \xi = \frac{\gamma}{\delta}, \quad \eta = \frac{1-\gamma}{\delta}. \tag{11}$$

where $\boldsymbol{B}(\xi,\eta)$ is the beta function. For the B_2 model in 1D slab geometry, the ansatz is taken as

$$w\mathcal{F}(\mu;\gamma,\delta)$$

where the parameters w, γ, and δ are given by consistency to the known moments.

We found that the 1D B_2 model shares the key features of the M_2 model in slab geometry, including existence of non-negative ansatz and therefore realizability, as well as global hyperbolicity. It is the focus of this paper to extend the 1D B_2 model to three-dimensional case.

Our motivation to this extension is based on observing a common attribute between the B_2 and the M_2 ansatz in 1D slab geometry. Both ansätze can exactly recover the isotropic distribution. At the same time, both ansätze tend towards a combination of Dirac functions as the corresponding moments approach the boundary of the realizability domain[4]. Dirac functions could not be recovered by the standard spectral method which has a polynomial as an ansatz. It has been pointed out that the inability to capture anisotropy is a drawback of the standard spectral method [9].

In three-dimensional space, the anisotropy of the specific intensity could come in orthogonal directions. For example, we consider a setup similar to the crossing beam problem discussed in [21] [5]. For the region $[x,y] \in [-1,1]\times[-1,1]$, consider equation (1) with the right-hand side chosen as isotropic scattering (which means σ_{s} is a non-negative constant):

$$\mathcal{C}(I) = \sigma_{\mathrm{s}}\left(-I + \frac{1}{4\pi}\langle I\rangle\right).$$

Laser beams are imposed as boundary inflow from orthogonal directions: $I = \delta(\boldsymbol{\Omega}\cdot\mathbf{e}_x - 1)$ on the boundary $x=-1$, and $I = \delta(\boldsymbol{\Omega}\cdot\mathbf{e}_y - 1)$ on the boundary $y = -1$.

For the extreme case when the medium is vacuum and $\sigma_{\mathrm{s}} = 0$, the exact solution for any $ct > 2$ is

$$I = \delta(\boldsymbol{\Omega}\cdot\mathbf{e}_x - 1) + \delta(\boldsymbol{\Omega}\cdot\mathbf{e}_y - 1). \tag{12}$$

It is pointed out in [21] that the closure of the set of M_2 ansatz contains the distribution in (12). We aim to construct an ansatz that can capture anisotropy in orthogonal directions, like the M_2 ansatz.

For non-vanishing scattering, the steady-state solution of the above problem is an isotropic distribution. For any period before steady-state is reached, the exact

[4]The focus of this study is formal derivation of the model and discussions on its limiting behaviour are not rigorous analysis.

[5]The crossing beam problem discussed in [21] could be seen as a 2D generalization of the double beam problem previously discussed in [4]. In [21], this example is used to demonstrate the advantage of the M_2 model over its first-order counterpart, the M_1 model.

specific intensity I should be somewhere between double beams, as in (12), and isotropic. The ansatz of the M_2 model provides a smooth interpolation between these two extremes, giving it an advantage in simulating such problems. We aim to propose an ansatz with similar features. This will be discussed in the following sections.

3. 3D B_2 Model

For second order models, which are the subject of this paper, the closure of the set of realizable moments as given in [16] is

$$\begin{aligned}\mathcal{M} = \Big\{ \big(E^0, \mathbf{E}^1, \mathbf{E}^2\big) \in \mathbb{R} \times \mathbb{R}^3 \times \mathbb{R}^{3\times 3},\ \text{s.t. } 0 < E^0 = \text{Trace}(\mathbf{E}^2), \\ \|\mathbf{E}^1\| \le E^0,\ \text{and } E^0\mathbf{E}^2 - \mathbf{E}^1 \otimes \mathbf{E}^1 \text{ symmetric non-negative}\Big\}.\end{aligned} \tag{13}$$

It is also referred to as the realizability domain. Our goal is to reconstruct an ansatz of the specific intensity given moments within $\mathcal{M}$.

3.1. General Formulation of the Ansatz. In this subsection, we propose a general formulation of the ansatz for the specific intensity and discuss consistency requirements. We take the summation of three axisymmetric distributions as the ansatz for the specific intensity:

$$\hat{I}_B(\mathbf{\Omega}) = \sum_{i=1}^{3} \frac{1}{2\pi} w_i f(\mathbf{\Omega}\cdot\mathbf{R}_i; \gamma_i, \delta_i), \tag{14}$$

where $\mathbf{R}_i$ are three mutually orthogonal unit vectors. We assume that the matrix $\boldsymbol{R} = [\mathbf{R}_1, \mathbf{R}_2, \mathbf{R}_3]$ satisfy $det(\boldsymbol{R}) = 1$. It is also assumed that $f(\mu;\gamma,\delta)$ is a non-negative function of μ with two shape parameters γ and δ, and $\int_{-1}^{1} f(\mu;\gamma,\delta)\,\mathrm{d}\mu = 1$. All the parameters in the ansatz, including $\mathbf{R}_i$, w_i, γ_i, and δ_i, $i = 1,2,3$, are functions of known moments and are independent of $\mathbf{\Omega}$. In this subsection, we discuss the properties of (14) for any arbitrary non-negative function $f(\mu;\gamma,\delta)$ whose integral over $\mu \in [-1,1]$ is one. To simplify the computing process in discussing the consistency conditions, we first make the following observation which will be used later. The proof of the following lemma is by straightforward calculation and will be omitted here.

Lemma 3.1. *For any permutation l, m, k of $1,2,3$, $\forall n_l, n_m, n_k \in \mathbb{N}$, we have*

$$\langle (\mathbf{\Omega}\cdot\mathbf{R}_l)^{n_l} (\mathbf{\Omega}\cdot\mathbf{R}_m)^{n_m} (\mathbf{\Omega}\cdot\mathbf{R}_k)^{n_k} f(\mathbf{\Omega}\cdot\mathbf{R}_k;\gamma_k,\delta_k)\rangle = \begin{cases} 0, \text{ if either } n_l \text{ or } n_m \text{ is odd}, \\[2ex] 2\pi \int_{-1}^{1} \mu^{n_k} f(\mu;\gamma_k,\delta_k)\,\mathrm{d}\mu, \text{ if } n_l = n_m = 0, \\[2ex] \pi \int_{-1}^{1} (1-\mu^2)\mu^{n_k} f(\mu;\gamma_k,\delta_k)\,\mathrm{d}\mu, \text{ if } n_l = 2,\ n_m = 0. \end{cases}$$

Take $\mathbf{v}$ as defined in (3), the moments of interest are

$$\mathbf{E} = [E^0, E^1_1, E^1_2, E^1_3, E^2_{11}, E^2_{12}, E^2_{13}, E^2_{22}, E^2_{23}]^T = \int_{\mathbb{S}^2} \mathbf{v} \hat{I}_B \,\mathrm{d}\mathbf{\Omega}.$$

The moment system based on the ansatz (14) is derived as

$$\frac{\partial \mathbf{E}}{\partial t} + \frac{\partial \mathbf{f}_x(\mathbf{E})}{\partial x} + \frac{\partial \mathbf{f}_y(\mathbf{E})}{\partial y} + \frac{\partial \mathbf{f}_z(\mathbf{E})}{\partial z} = \mathbf{r}(\mathbf{E}), \tag{15}$$

where

$$\mathbf{f}_x = [E^1_1, E^2_{11}, E^2_{12}, E^2_{13}, E^3_{111}, E^3_{112}, E^3_{113}, E^3_{122}, E^3_{123}]^T = \int_{\mathbb{S}^2} (\mathbf{\Omega}\cdot\mathbf{e}_x)\mathbf{v}\hat{I}_B \,\mathrm{d}\mathbf{\Omega},$$
$$\mathbf{f}_y = [E^1_2, E^2_{21}, E^2_{22}, E^2_{23}, E^3_{211}, E^3_{212}, E^3_{213}, E^3_{222}, E^3_{223}]^T = \int_{\mathbb{S}^2} (\mathbf{\Omega}\cdot\mathbf{e}_y)\mathbf{v}\hat{I}_B \,\mathrm{d}\mathbf{\Omega},$$
$$\mathbf{f}_z = [E^1_3, E^2_{31}, E^2_{32}, E^2_{33}, E^3_{311}, E^3_{312}, E^3_{313}, E^3_{322}, E^3_{323}]^T = \int_{\mathbb{S}^2} (\mathbf{\Omega}\cdot\mathbf{e}_z)\mathbf{v}\hat{I}_B \,\mathrm{d}\mathbf{\Omega},$$

and $\mathbf{r}(\mathbf{E})$ is calculated from the scattering term, which is out of the scope of our interests in this paper.

The parameters $\mathbf{R}_i$, w_i, γ_i, and δ_i have to satisfy the consistency conditions:

$$E^0 = \left\langle \hat{I}_B \right\rangle, \quad \mathbf{E}^1 = \left\langle \mathbf{\Omega}\hat{I}_B \right\rangle, \quad \text{and} \quad \mathbf{E}^2 = \left\langle \mathbf{\Omega}\otimes\mathbf{\Omega}\hat{I}_B \right\rangle. \tag{16}$$

The vectors $\mathbf{R}_i$ in (14) are determined by the consistency conditions (16) instantly, as shown in the following lemma.

Lemma 3.2. *The consistency constraints* (16) *require that* $\mathbf{R}_j$*,* $j = 1,2,3$*, be the eigenvectors of* $\mathbf{E}^2$.

Proof. Let $\boldsymbol{R} = [\mathbf{R}_1, \mathbf{R}_2, \mathbf{R}_3]$. As $\boldsymbol{R}$ is an orthogonal matrix, we have $\boldsymbol{R}^{-1} = \boldsymbol{R}^T$. To prove the lemma, it suffices to show that

$$\mathbf{R}_j^T\mathbf{E}^2\mathbf{R}_i = \left\langle (\mathbf{\Omega}\cdot\mathbf{R}_j)(\mathbf{\Omega}\cdot\mathbf{R}_i)\hat{I}_B \right\rangle = 0, \quad \text{if } j \neq i. \tag{17}$$

The reason is that (17) would indicate that $\boldsymbol{R}^{-1}\mathbf{E}^2\boldsymbol{R}$ is a diagonal matrix, and therefore $\mathbf{R}_j$, $j = 1,2,3$, are the eigenvectors of $\mathbf{E}^2$.

In order to prove (17), consider the case $j = 1$, $i = 2$,

$$\mathbf{R}_1^T\mathbf{E}^2\mathbf{R}_2 = \left\langle (\mathbf{\Omega}\cdot\mathbf{R}_1)(\mathbf{\Omega}\cdot\mathbf{R}_2)\hat{I}_B \right\rangle = \frac{1}{2\pi}\int_{\mathbb{S}^2} (\mathbf{\Omega}\cdot\mathbf{R}_1)(\mathbf{\Omega}\cdot\mathbf{R}_2)\sum_{i=1}^3 w_i f(\mathbf{\Omega}\cdot\mathbf{R}_i;\gamma_i,\delta_i)\,\mathrm{d}\mathbf{\Omega}.$$

By Lemma 3.1,

$$\int_{\mathbb{S}^2} (\mathbf{\Omega}\cdot\mathbf{R}_1)(\mathbf{\Omega}\cdot\mathbf{R}_2) w_k f(\mathbf{\Omega}\cdot\mathbf{R}_k;\gamma_k,\delta_k)\,\mathrm{d}\mathbf{\Omega} = 0, \quad k = 1,2,3.$$

Therefore $\mathbf{R}_1^T\mathbf{E}^2\mathbf{R}_2 = 0$. Similar arguments show that $\mathbf{R}_1^T\mathbf{E}^2\mathbf{R}_3 = \mathbf{R}_2^T\mathbf{E}^2\mathbf{R}_3 = 0$. □

With the parameters $\mathbf{R}_i$ determined, we now consider the consistency requirements under the coordinate system $(\mathbf{R}_1, \mathbf{R}_2, \mathbf{R}_3)$. In this coordinate system, $\mathbf{E}^2$ is a diagonal matrix. Also, as Lemma 3.2 specify $\mathbf{R}_j$, $j = 1,2,3$, to be the eigenvectors of $\mathbf{E}^2$, we only need to look at the consistency of E^0, $\mathbf{E}^1$, and all the eigenvalues of $\mathbf{E}^2$ and all other constraints of consistency of the moments are naturally satisfied. This leaves us with 6 constraints. On the other hand, with $\mathbf{R}_j$, $j = 1,2,3$ fixed, there are 9 parameters in the ansatz (14). Denote

$$\sigma_i = w_i \int_{-1}^1 \mu^2 f(\mu;\gamma_i,\delta_i)\,\mathrm{d}\mu. \tag{18}$$

Once σ_i, $i = 1,2,3$ are specified, then direct calculation shows w_i for $i = 1,2,3$ would be determined by consistency constraints, as specified in the following lemma.

Lemma 3.3. *Let* λ_i *be the eigenvalue corresponding to* $\mathbf{R}_i$*. Then* w_i*,* σ_i *and* λ_i *satisfy the following constraints:*

$$\begin{aligned} w_1 &= 2\sigma_1 - (\sigma_2+\sigma_3) - \lambda_1 + \lambda_2 + \lambda_3, \\ w_2 &= 2\sigma_2 - (\sigma_1+\sigma_3) - \lambda_2 + \lambda_1 + \lambda_3, \\ w_3 &= 2\sigma_3 - (\sigma_1+\sigma_2) - \lambda_3 + \lambda_1 + \lambda_2. \end{aligned} \tag{19}$$

Once w_i, $i = 1, 2, 3$, are given, consistency requires that γ_i and δ_i satisfy

$$w_i \int_{-1}^{1} \mu f(\mu; \gamma_i, \delta_i)\, \mathrm{d}\mu = F_i, \tag{20}$$

where $F_i = \mathbf{E}^1 \cdot \mathbf{R}_i$. If $w_i = 0$, then the term $w_i f(\mathbf{\Omega} \cdot \mathbf{R}_i; \gamma_i, \delta_i)$ does not appear in the ansatz (14). From now on we assume $w_i \neq 0$. Recall that by definition, the function $f(\mu; \gamma, \delta)$ is a non-negative distribution on $\mu \in [-1, 1]$, and its zeroth moment is 1. Moreover, the first and second-order moments of f are respectively $\dfrac{F_i}{w_i}$ and $\dfrac{\sigma_i}{w_i}$. So, combining (18) and (20) define a 1D moment problem. This means that once the value of the three parameters σ_i, $i = 1, 2, 3$ are specified, the consistency condition (16) could be decomposed into three decoupled 1D moment problems

$$\begin{cases} \int_{-1}^{1} \mu f(\mu; \gamma_i, \delta_i)\, \mathrm{d}\mu = \dfrac{F_i}{w_i}, \\ \int_{-1}^{1} \mu^2 f(\mu; \gamma_i, \delta_i)\, \mathrm{d}\mu = \dfrac{\sigma_i}{w_i}, \end{cases} \tag{21}$$

for $i = 1, 2, 3$.

In summary, we take (14) as the ansatz of the 3D B_2 model. Consistency requirements specify that R_j, $j = 1, 2, 3$, be the three eigenvectors of the second order moment tensor $\mathbf{E}^2$. The three free parameters in the ansatz are σ_i, $i = 1, 2, 3$. The issues of choosing the specific form of the function f and specifying σ_i, $i = 1, 2, 3$, will be discussed in Section 3.3 and Section 3.4, respectively. Once they are given, all the parameters in (14) are determined by solving the three decoupled 1D moment problems (21). In the next subsection, we will look at the behavior of the general ansatz (14) on the boundary of the realizability domain.

3.2. Realizability Domain. This subsection focuses on the ansatz $\hat{I}_B$ on the boundary of the realizability domain, which can be interpreted as the limit of a sequence of 3D B_2 ansätze. In the following discussions, we avoid the technicalities and the distributions we consider formally include the cases of combinations of Dirac functions. We shall discuss the existence of non-negative $\hat{I}_B$. According to [6], the realizability domains of the 1D moment problems in (21) are:

$$\left(\frac{F_i}{w_i} \right)^2 \leq \frac{\sigma_i}{w_i} \leq 1, \quad i = 1, 2, 3. \tag{22}$$

A sufficient condition for the existence of non-negative ansatz $\hat{I}_B$ is $w_i \geq 0$, $i = 1, 2, 3$. It follows that a non-negative ansatz $\hat{I}_B$ exists under the following conditions:

$$\left(\frac{F_i}{w_i} \right)^2 \leq \frac{\sigma_i}{w_i} \leq 1, \quad w_i \geq 0, \quad i = 1, 2, 3. \tag{23}$$

One would like to give a non-negative ansatz for as large a part of the realizability domain as possible to have a realizable closure. Before examining the non-negativity of the ansatz (14), we give the following result, which is an alternative characterization of the realizable moments:

Lemma 3.4. *Let $\{\lambda_j, \mathbf{R}_j\}$, $j = 1, 2, 3$, be the eigenpairs of $\mathbf{E}^2$, and $F_j = \mathbf{E}^1 \cdot \mathbf{R}_j$. Then the realizability domain $\mathcal{M}$ given by* (13) *is*

$$\mathcal{M} = \left\{ \left(E^0, \mathbf{E}^1, \mathbf{E}^2 \right) \,\middle|\, 0 < \sum_{i=1}^{3} \lambda_i = E^0,\ \sum_{i=1}^{3} \frac{F_i^2}{\lambda_i} \leq E^0 \right\}. \tag{24}$$

In (24)*, the term* $\dfrac{F_i^2}{\lambda_i} = 0$ *is taken to be zero if* $\lambda_i = 0$*.*

Proof. Denote the normalized first and second-order moments by $\hat{\mathbf{E}}^1 = \dfrac{\mathbf{E}^1}{E^0}$ and $\hat{\mathbf{E}}^2 = \dfrac{\mathbf{E}^2}{E^0}$. Let

$$\Lambda = \operatorname{diag}\left\{\frac{\lambda_1}{E^0}, \frac{\lambda_2}{E^0}, \frac{\lambda_3}{E^0}\right\}, \quad \Lambda^{\frac{1}{2}} = \operatorname{diag}\left\{\sqrt{\frac{\lambda_1}{E^0}}, \sqrt{\frac{\lambda_2}{E^0}}, \sqrt{\frac{\lambda_3}{E^0}}\right\},$$

and denote

$$\boldsymbol{R} = [\mathbf{R}_1, \mathbf{R}_2, \mathbf{R}_3], \quad \mathbf{T} = \Lambda^{\frac{1}{2}}\boldsymbol{R}.$$

Then

$$\hat{\mathbf{E}}^2 = \boldsymbol{R}^T \Lambda \boldsymbol{R} = \mathbf{T}^T\mathbf{T}.$$

Assuming that $\lambda_i \neq 0$, $i = 1,2,3$. Then non-negativity of the matrix $\hat{\mathbf{E}}^2 - \hat{\mathbf{E}}^1 \otimes \hat{\mathbf{E}}^1$ is equivalent to the non-negativity of the matrix $\boldsymbol{I} - \mathbf{T}^{-T}\hat{\mathbf{E}}^1(\hat{\mathbf{E}}^1)^T\mathbf{T}^{-1}$, which, in turn, is equivalent to $\|(\hat{\mathbf{E}}^1)^T\mathbf{T}^{-1}\|_2 \leq 1$, and therefore equivalent to

$$\sum_{i=1}^{3} \frac{F_i^2}{\lambda_i} \leq E^0. \tag{25}$$

The cases when there exists i for which $\lambda_i = 0$ can be proved by entirely similar arguments. $\square$

Remark 3.1. *The above lemma could also be proved by applying the method for solving modified eigenvalue problems proposed in* [28]*.*

Making use of Lemma 3.4, the realizability domain can be visualized as: take any point inside a triangle and let $\left(\dfrac{\lambda_1}{E^0}, \dfrac{\lambda_2}{E^0}, \dfrac{\lambda_3}{E^0}\right)$ be its barycentric coordinates. Then the corresponding (F_1, F_2, F_3) lie in the ellipsoid (25). Different points inside the triangle correspond to different ellipsoids.

Each side of the triangle corresponds to the cases where at least one eigenvalue of $\mathbf{E}^2$ vanishes. In such cases non-negativity of $\hat{I}_B$ given in (14) would impose the following constraints on the first and second-order moments:

Lemma 3.5. *The non-negativity of the ansatz* $\hat{I}_B$ *requires that if there exists* $i = 1,2$ *or* 3 *such that* $\lambda_i = 0$*, then*

$$\begin{cases} F_i = 0 \ \textit{and} \ \sigma_i = 0, \\ |F_j| \leq \sigma_j \leq \lambda_j, \quad \textit{for} \ \forall j \neq i. \end{cases}$$

Proof. Consider the case $i = 1$. Since

$$0 = \lambda_1 = \int_{\mathbb{S}^2} (\mathbf{\Omega} \cdot \mathbf{R}_1)^2 \hat{I}_B(\mathbf{\Omega}) \,\mathrm{d}\mathbf{\Omega}, \tag{26}$$

then $\hat{I}_B$ can only be non-zero when $\mathbf{\Omega} \cdot \mathbf{R}_1 = 0$. This gives

$$F_1 = \int_{\mathbb{S}^2} (\mathbf{\Omega} \cdot \mathbf{R}_1) \hat{I}_B(\mathbf{\Omega}) \,\mathrm{d}\mathbf{\Omega} = 0.$$

To prove $\sigma_1 = 0$, let us study two cases.

(1) For $w_1 = 0$, it can be seen from (18) that $\sigma_1 = 0$.
(2) If $w_1 \neq 0$. Recall that $\hat{I}_B$ can only be non-zero when $\mathbf{\Omega} \cdot \mathbf{R}_1 = 0$. Then (18) shows $\sigma_1 = 0$.

Next, we show that $\sigma_j \geq |F_j|$, $j = 2,3$. We look at two cases.

(1) In the case that $w_j = 0$, by (20) we have $F_j = 0$, and by (18) we see that $\sigma_j = 0$. Hence $\sigma_j \geq |F_j|$.

(2) If $w_j \neq 0$. Again, note that $\hat{I}_B$ can only be non-zero when $\mathbf{\Omega} \cdot \mathbf{R}_1 = 0$, therefore for $j \neq 1$, the function $f(\mathbf{\Omega} \cdot \mathbf{R}_j; \gamma_j, \delta_j)$ has the form

$$f(\mathbf{\Omega} \cdot \mathbf{R}_j; \gamma_j, \delta_j) = \alpha_j^- \delta(\mathbf{\Omega} \cdot \mathbf{R}_j + 1) + \alpha_j^+ \delta(\mathbf{\Omega} \cdot \mathbf{R}_j - 1).$$

From (18) we know that in such cases $\sigma_j = w_j$. Combine this with the left inequality in (23), and we have $\sigma_j \geq |F_j|$.

Finally, we prove $\sigma_j \leq \lambda_j$, $j = 2,3$. Plugging $\sigma_1 = \lambda_1 = 0$ into (19) gives

$$\sigma_2 - \sigma_3 = \lambda_2 - \lambda_3,$$

and

$$\sigma_2 + \sigma_3 = \lambda_2 + \lambda_3 - w_1,$$

If $\hat{I}_B$ is non-negative, then $w_1 \geq 0$. Combine the above and notice that $\lambda_2 + \lambda_3 = E^0$, we have

$$\sigma_j \leq \lambda_j, \quad j = 2,3.$$

The proofs for $i = 2,3$, follows in a similar manner. □

Remark 3.2. *As a special case of Lemma 3.5, if there exists j such that $\lambda_j = E^0$, and $\lambda_i = 0$ for $i \neq j$, then*

$$\begin{cases} |F_j| \leq \sigma_j \leq \lambda_j = E^0, \\ F_i = 0 \text{ and } \sigma_i = 0, \quad \text{for } \forall i \neq j. \end{cases}$$

From Lemma 3.5, it is clear that when $\lambda_i = 0$ is the only zero eigenvalue of $\mathbf{E}^2$, the region for which the ansatz (14) admits a non-negative distribution is limited to the rectangle $|F_j| \leq \lambda_j$, $j \neq i$. We point out that this rectangle can cover only 4 points for the boundary of the realizability domain in (25), which in this case becomes the ellipse

$$\frac{F_j^2}{\lambda_j} + \frac{F_k^2}{\lambda_k} = E^0, \quad j \neq k.$$

For other boundary moments, we have the following result:

Lemma 3.6. *Suppose $\lambda_i > 0$, $i = 1,2,3$. Then on the boundary of the realizability domain, where*

$$\frac{F_1^2}{\lambda_1} + \frac{F_2^2}{\lambda_2} + \frac{F_3^2}{\lambda_3} = E^0, \tag{27}$$

there are only two kinds of moments for which $\hat{I}_B$ can be non-negative:

(1) *$\exists i$, such that $\lambda_i = \frac{F_i^2}{E^0}$. Meanwhile for $j,k \neq i$, the relationships $\lambda_j = \lambda_k$ and $F_j = F_k = 0$ hold.*

(2) *$\forall j = 1,2,3$, the constraint $|F_j| = \lambda_j$ is satisfied.*

Proof. Let the covariance matrix of the distribution function be

$$\boldsymbol{V} = \frac{\mathbf{E}^2}{E^0} - \left(\frac{\mathbf{E}^1}{E^0}\right)\left(\frac{\mathbf{E}^1}{E^0}\right)^T.$$

If

$$\frac{F_1^2}{\lambda_1} + \frac{F_2^2}{\lambda_2} + \frac{F_3^2}{\lambda_3} = E^0,$$

then there exists at least one zero eigenvalue for $\boldsymbol{V}$. Denote the corresponding eigenvector by $\mathbf{U}$, and [16] has shown that any non-negative distribution could be non-zero only when $\boldsymbol{\Omega}\cdot\mathbf{U} = \frac{1}{E^0}(\mathbf{E}^1\cdot\mathbf{U})$. We will repeatedly make use of this fact in the following discussions.

We study the two possible cases:

(1) Suppose $\mathbf{U}$ is aligned with some eigenvector of $\mathbf{E}^2$. Without loss of generality, we assume $\mathbf{R}_3//\mathbf{U}$. Then a non-negative distribution could be non-zero only on $\boldsymbol{\Omega}\cdot\mathbf{R}_3 = \frac{F_3}{E^0}$. In addition,

$$0 = \mathbf{U}^T\boldsymbol{V}\mathbf{U} = \mathbf{R}_3^T\left[\frac{1}{E^0}\mathbf{E}^2 - \left(\frac{\mathbf{E}^1}{E^0}\right)\left(\frac{\mathbf{E}^1}{E^0}\right)^T\right]\mathbf{R}_3 = \frac{\lambda_3}{E^0} - \left(\frac{F_3}{E^0}\right)^2, \tag{28}$$

which gives $\lambda_3 = \frac{F_3^2}{E^0}$. If $F_3 = 0$ then $\lambda_3 = 0$, which has been ruled out in our assumptions. So $F_3 \neq 0$, which means a non-negative distribution (14) can only be

$$\hat{I}_B = \frac{E^0}{2\pi}\delta\left(\boldsymbol{\Omega}\cdot\mathbf{R}_3 - \frac{F_3}{E^0}\right). \tag{29}$$

Therefore $w_1 = w_2 = 0$, and by (18) and (20) we would have $\sigma_1 = \sigma_2 = F_1 = F_2 = 0$. Substituting this into (19) gives $\lambda_1 = \lambda_2 = \frac{1}{2}(w_3 - \lambda_3)$. Conversely, moments satisfying $\lambda_1 = \lambda_2$ and $F_1 = F_2 = 0$ in addition to $\lambda_3 = \frac{F_3^2}{E^0}$ could be generated by the ansatz (29).

(2) Consider the case when $\mathbf{U}$ is not aligned to any $\mathbf{R}_j$. The only way to give a non-negative distribution for (14) in this case is

$$\hat{I}_B = \sum_{i=1}^{3}[\alpha_i^+\delta(\boldsymbol{\Omega}\cdot\mathbf{R}_i - 1) + \alpha_i^-\delta(\boldsymbol{\Omega}\cdot\mathbf{R}_i + 1)].$$

Hence $\sigma_j = w_j$, $j = 1,2,3$. Combining these with (19) gives $\sigma_j = \lambda_j$, $j = 1,2,3$. But condition (23) require

$$|F_j| \le \lambda_j, \quad j = 1,2,3. \tag{30}$$

Recall assumption (27), and notice

$$E^0 = \frac{F_1^2}{\lambda_1} + \frac{F_2^2}{\lambda_2} + \frac{F_3^2}{\lambda_3} \le \lambda_1 + \lambda_2 + \lambda_3 = E^0. \tag{31}$$

For all inequalities to hold, we need

$$|F_j| = \lambda_j,\ j = 1,2,3. \tag{32}$$

Conversely, for moments satisfying condition (32), choosing

$$\sigma_j = \lambda_j, \quad j = 1,2,3. \tag{33}$$

would give a non-negative ansatz.

The proof is completed. □

We are now clear about the cases where there exists a non-negative ansatz of the specific intensity on the boundary of the realizability domain. In Section 3.4, we will make use of this information in specifying the free parameters σ_i, $i = 1,2,3$. Before that, we will turn to specifying the formula for f in the next subsection.

3.3. Closure using B-distribution Ansatz. We take f to be the β distribution used in the B_2 ansatz for slab geometry

$$f(\mu;\gamma,\delta) = \mathcal{F}(\mu;\gamma,\delta), \quad \xi = \frac{\gamma}{\delta}, \quad \eta = \frac{1-\gamma}{\delta}, \tag{34}$$

where $\mathcal{F}$ is as defined in (11). This subsection derives closure relation of the moment model based on this type of ansatz.

Retaining only one term in (14) would provide the same ansatz as the one-dimensional B_2 ansatz which we studied previously [3]. Taking $\xi = \eta = 1$ in equation (34) would give f as a constant function. If either ξ or η approach zero, the limit of the function f is a Dirac function. If both of them go to zeros at a fixed rate, the function f will become a combination of two Dirac functions. This capacity of (34) to interpolate between the constant function and Dirac functions is a feature it shares with the M_2 ansatz. Also, for slab geometry, the B_2 model possesses numerous nice properties similar to the M_2 model; therefore, we use it as building blocks for three-dimensional ansatz.

If (34) is the distribution function f in (18) and (20), then for σ_i, w_i and F_i satisfying the realizability condition (22), we have

$$\xi_i \geq 0, \quad \eta_i \geq 0,$$

which gives an integrable function for (34). For the above cases, the parameters γ_i and δ_i are given as follow:

Lemma 3.7. *If* (23) *is fulfilled, we have*

$$\gamma_i = \frac{F_i + w_i}{2w_i} \quad \text{and} \quad \delta_i = -\frac{F_i^2 - \sigma_i w_i}{w_i^2 - \sigma_i w_i}, \quad \forall i = 1,2,3. \tag{35}$$

Proof. From the integration properties of the standard β distribution [13] it could be derived that

$$\int_{-1}^{1} \mu f(\mu;\gamma_i,\delta_i)\,\mathrm{d}\mu = 2\gamma_i - 1, \tag{36}$$

and

$$\int_{-1}^{1} \mu^2 f(\mu;\gamma_i,\delta_i)\,\mathrm{d}\mu = 4\frac{\gamma_i(\gamma_i - 1)}{1+\delta_i} + 1. \tag{37}$$

Combining (36), (37) with (18), (20) gives us (35). □

Note that (18), (20), and (19) together are the necessary and sufficient conditions for consistency constraints of all known moments. This leaves σ_i, $i = 1,2,3$, to be the three free parameters. We shall return to the problem of determining σ_i later. For the present, we assume σ_i, $i = 1,2,3$ are all given, and the following lemma gives the closure relationship of the B_2 model.

Lemma 3.8. *Let $\boldsymbol{R} = [\mathbf{R}_1, \mathbf{R}_2, \mathbf{R}_3] \in \mathbb{R}^{3\times 3}$, and denote by R_{ij} the entries of the matrix $\boldsymbol{R}$, the flux closure is then given by $\mathbf{f}(E^0, \mathbf{E}^1, \mathbf{E}^2)$, which relies on $\mathbf{E}^1$, $\mathbf{E}^2$ and $\mathbf{E}^3$, with $\mathbf{E}^3$ given as*

$$E^3_{ijk} = \left\langle (\boldsymbol{\Omega}\cdot\mathbf{R}_l)(\boldsymbol{\Omega}\cdot\mathbf{R}_m)(\boldsymbol{\Omega}\cdot\mathbf{R}_n)\hat{I}_B \right\rangle R_{il}R_{jm}R_{kn},$$

where the Einstein summation convention is used. For distribution ansatz $\hat{I}_B$ given by (14),

$$\left\langle(\mathbf{\Omega}\cdot\mathbf{R}_l)(\mathbf{\Omega}\cdot\mathbf{R}_m)(\mathbf{\Omega}\cdot\mathbf{R}_n)\hat{I}_B\right\rangle = \tag{38}$$
$$\begin{cases} \dfrac{F_l(\sigma_l^2+2F_l^2-3w_l\sigma_l)}{2F_l^2-w_l\sigma_l-w_l^2}, & \text{if } l=m=n, \\ \dfrac{F_l}{2}\left(1-\dfrac{\sigma_l^2+2F_l^2-3w_l\sigma_l}{2F_l^2-w_l\sigma_l-w_l^2}\right), & \text{if } m=n,\ m\neq l, \\ 0, & \text{if } l\neq m\neq n. \end{cases}$$

Proof. Consider the case when $l=m=n=1$ at first. By Lemma 3.1,

$$\begin{aligned}\left\langle(\mathbf{\Omega}\cdot\mathbf{R}_l)(\mathbf{\Omega}\cdot\mathbf{R}_m)(\mathbf{\Omega}\cdot\mathbf{R}_n)\hat{I}_B\right\rangle &= \frac{1}{2\pi}\int_{\mathbb{S}^2}(\mathbf{\Omega}\cdot\mathbf{R}_1)^3\sum_{i=1}^{3}w_i f(\mathbf{\Omega}\cdot\mathbf{R}_i;\gamma_i,\delta_i)\,\mathrm{d}\mathbf{\Omega} \\ &= w_1\int_{-1}^{1}\mu^3 f(\mu;\gamma_1,\delta_1)\,\mathrm{d}\mu.\end{aligned}$$

From the integration properties of the standard β distribution [13] it could be derived that

$$\int_{-1}^{1}\mu^3 f(\mu;\gamma_1,\delta_1)\,\mathrm{d}\mu = \frac{(\xi_1-\eta_1)(\xi_1^2-2\xi_1\eta_1+3\xi_1+\eta_1^2+3\eta_1+2)}{(\xi_1+\eta_1)(\xi_1+\eta_1+1)(\xi_1+\eta_1+2)}.$$

Recall (34) and Lemma 3.7 for the values of ξ_1 and η_1, we have

$$\int_{-1}^{1}\mu^3 f(\mu;\gamma_1,\delta_1)\,\mathrm{d}\mu = \frac{F_1(\sigma_1^2+2F_1^2-3w_1\sigma_1)}{2F_1^2-w_1\sigma_1-w_1^2}.$$

For $l=m=n=2$ or $l=m=n=3$ the computation is similar.

Now consider the case when $m=n$, $m\neq l$. Suppose $m=n=1$ and $l=2$. It could be proved by direct computation that

$$\left\langle(\mathbf{\Omega}\cdot\mathbf{R}_1)^2(\mathbf{\Omega}\cdot\mathbf{R}_2)\hat{I}_B\right\rangle = \left\langle(\mathbf{\Omega}\cdot\mathbf{R}_3)^2(\mathbf{\Omega}\cdot\mathbf{R}_2)\hat{I}_B\right\rangle.$$

On the other hand,

$$\left\langle(\mathbf{\Omega}\cdot\mathbf{R}_1)^2(\mathbf{\Omega}\cdot\mathbf{R}_2)\hat{I}_B\right\rangle+\left\langle(\mathbf{\Omega}\cdot\mathbf{R}_3)^2(\mathbf{\Omega}\cdot\mathbf{R}_2)\hat{I}_B\right\rangle+\left\langle(\mathbf{\Omega}\cdot\mathbf{R}_2)^3\hat{I}_B\right\rangle = \left\langle(\mathbf{\Omega}\cdot\mathbf{R}_2)\hat{I}_B\right\rangle = F_2.$$

It follows that

$$\left\langle(\mathbf{\Omega}\cdot\mathbf{R}_1)^2(\mathbf{\Omega}\cdot\mathbf{R}_2)\hat{I}_B\right\rangle = \left\langle(\mathbf{\Omega}\cdot\mathbf{R}_3)^2(\mathbf{\Omega}\cdot\mathbf{R}_2)\hat{I}_B\right\rangle = \frac{F_2}{2}\left(1-\frac{\sigma_2^2+2F_2^2-3w_2\sigma_2}{2F_2^2-w_2\sigma_2-w_2^2}\right).$$

Also, by Lemma 3.1,

$$\int_{\mathbb{S}^2}(\mathbf{\Omega}\cdot\mathbf{R}_1)(\mathbf{\Omega}\cdot\mathbf{R}_2)(\mathbf{\Omega}\cdot\mathbf{R}_3)w_j f(\mathbf{\Omega}\cdot\mathbf{R}_j;\gamma_j,\delta_j)\,\mathrm{d}\mathbf{\Omega} = 0, \quad j=1,2,3.$$

Therefore,

$$\left\langle(\mathbf{\Omega}\cdot\mathbf{R}_1)(\mathbf{\Omega}\cdot\mathbf{R}_2)(\mathbf{\Omega}\cdot\mathbf{R}_3)\hat{I}_B\right\rangle = 0.$$

Summarizing the results from the above three cases completes the proof of this lemma. □

In brief summary, when taking f to be β distributions, the moment model is fully determined by lemma 3.8 once σ_i, $i=1,2,3$, are given. In the next subsection, we discuss the choice of σ_i, $i=1,2,3$.

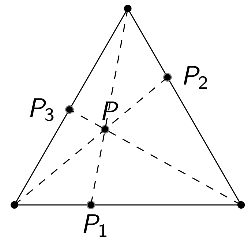

FIGURE 1. Schematic diagram of the interpolation.

3.4. Free Parameters σ_i. It remains to give σ_i, $i = 1, 2, 3$. Note that the trace of the matrix $\mathbf{E}^2$ equals E^0, so λ_i satisfy the constraint

$$\lambda_1 + \lambda_2 + \lambda_3 = E^0.$$

And due to the positive semi-definiteness of $\mathbf{E}^2$, we have $\lambda_i \geq 0$, $i = 1, 2, 3$. This allows us to regard $\left(\frac{\lambda_1}{E^0}, \frac{\lambda_2}{E^0}, \frac{\lambda_3}{E^0}\right)$ as the barycentric coordinates of a point $\mathbf{P}$ within a triangle (see Figure 1). At the vertices of this triangle, only one of the three eigenvalues of $\mathbf{E}^2$ is non-zero. By the similar arguments in the proof of Lemma 3.5, a non-negative $\hat{I}_B$ in such cases retains only one of its three terms. Combining this fact with (19) gives us the closure at the vertices of the triangle:

$$\begin{array}{ccc} \left(\frac{\lambda_1}{E^0}, \frac{\lambda_2}{E^0}, \frac{\lambda_3}{E^0}\right) & \mapsto & (\sigma_1, \sigma_2, \sigma_3) \\ (1,0,0) & & (E_0, 0, 0) \\ (0,1,0) & & (0, E_0, 0) \\ (0,0,1) & & (0, 0, E_0) \end{array}$$

Now that the value of $(\sigma_1, \sigma_2, \sigma_3)$ at the vertices are specified by the closure relation, we are to propose a smooth extension of the functions σ_i at the vertices to the whole triangle, then a smooth extension of the closure relation is achieved. A natural extension is a scaled identity map as

$$\left(\frac{\lambda_1}{E^0}, \frac{\lambda_2}{E^0}, \frac{\lambda_3}{E^0}\right) \mapsto (\lambda_1, \lambda_2, \lambda_3),$$

However, by (19) this extension results in $w_j = \sigma_j$. As a consequence, the ansatz would always be linear combinations of Dirac functions. It cannot include any smooth functions, particularly it cannot recover a constant distribution at the equilibrium. Moreover, such an extension does not depend on the first-order moments F_i at all, which is definitely not appropriate. This motivates us to seek other ways of extending.

To figure out an appropriate extension, we assume it takes the following general but decomposed form

$$\sigma_i = \sum_{j=1}^{3} s_j \sigma_i^j, \quad i = 1, 2, 3. \tag{39}$$

It is assumed that s_j is a weight function that relies only on λ_j, and σ_i^j is a function that depends on both the first-order moments and the eigenvalues of the second-order moments but that is independent of λ_j.

First, we determine the values of the weights, s_j. Our approach is motivated by geometric considerations. It is illustrated in Figure 1. For the point $\mathbf{P}$, we connect each vertex to $\mathbf{P}$ and extend the line segment until it intersects with the opposite side. Those three intersection points are denoted $\mathbf{P}_j$, $j = 1, 2, 3$, where the index j indicates that $\mathbf{P}_j$ lies on the side where $\lambda_j = 0$. Denote the barycentric coordinates of $\mathbf{P}_j$ by $\mathbf{P}_j = \left(\frac{\lambda_1^j}{E^0}, \frac{\lambda_2^j}{E^0}, \frac{\lambda_3^j}{E^0} \right)$. Therefore,

$$\lambda_i = \sum_{j=1}^{3} s_j \lambda_i^j, \quad j = 1, 2, 3,$$

where

$$s_1 = \frac{1}{2}(\lambda_2 + \lambda_3), \quad s_2 = \frac{1}{2}(\lambda_1 + \lambda_3), \quad s_3 = \frac{1}{2}(\lambda_1 + \lambda_2). \tag{40}$$

The functions in (40) are used as the weights s_j, $j = 1, 2, 3$.

The next thing is to specify σ_i^j. Consider a 3×3 matrix with the nine functions, $\sigma_i^j \left(\frac{\lambda_1}{E^0}, \frac{\lambda_2}{E^0}, \frac{\lambda_3}{E^0}; \frac{F_1}{E^0}, \frac{F_2}{E^0}, \frac{F_3}{E^0} \right)$, $i, j = 1, 2, 3$, as its elements. Naturally, one would expect σ_i^j to have symmetry in the permutation of indices. Precisely, if τ is a permutation on the index set $\{1, 2, 3\}$, then for $\forall i, j = 1, 2, 3$,

$$\sigma_i^j \left(\frac{\lambda_1}{E^0}, \frac{\lambda_2}{E^0}, \frac{\lambda_3}{E^0}; \frac{F_1}{E^0}, \frac{F_2}{E^0}, \frac{F_3}{E^0} \right) = \sigma_{\tau(i)}^{\tau(j)} \left(\frac{\lambda_{\tau(1)}}{E^0}, \frac{\lambda_{\tau(2)}}{E^0}, \frac{\lambda_{\tau(3)}}{E^0}; \frac{F_{\tau(1)}}{E^0}, \frac{F_{\tau(2)}}{E^0}, \frac{F_{\tau(3)}}{E^0} \right).$$

Thus, we have only two functions for all σ_i^j:

- The three diagonal entries, σ_i^i, $i = 1, 2, 3$, have the same form;
- All six off-diagonal entries, σ_i^j, $i \neq j$, have the same form.

Since σ_i^j is assumed to be independent of λ_j, it should be constant on the line segment $\mathbf{PP}_j$. As an example, since σ_i^1 does not depend on λ_1, it should be independent of $\lambda_2 + \lambda_3$. Therefore, one may use $\frac{\lambda_2}{\lambda_2 + \lambda_3}$ and $\frac{\lambda_3}{\lambda_2 + \lambda_3}$ to replace λ_2 and λ_3 as variables in σ_i^1. Noticing that $\left(0, \frac{\lambda_2}{\lambda_2 + \lambda_3}, \frac{\lambda_3}{\lambda_2 + \lambda_3} \right)$ is the barycentric coordinate of $\mathbf{P}_1$, we thus have $\sigma_i^1\big|_{\mathbf{P}} = \sigma_i^1\big|_{\mathbf{P}_1}$, and it is constant on line $\mathbf{PP}_1$.

Moreover, this makes us assume σ_i^j is also independent of F_j. The reason is as follows. By Lemma 3.5, the only region in which (14) might have a non-negative distribution when $\lambda_j = 0$ is the rectangle $|F_k| \leq \lambda_k$, $k \neq j$. Therefore, even when all three λ_j, $j = 1, 2, 3$, are positive, we restrict our expected region to have a non-negative distribution inside the box $|F_k| \leq \lambda_k$, $k = 1, 2, 3$. Note that this domain of F_j depend on λ_j while σ_i^j does not rely on λ_j, so we are induced to let σ_i^j to be independent of F_j.

We proceed to specify σ_i^j by constraints at vertices and sides of the triangle. We first investigate the vertices to conclude that

Lemma 3.9. *With the assumptions above on σ_i^j, we have*

$$\sigma_i^i \equiv 0, \quad i = 1, 2, 3.$$

Proof. First, take the vertex in which $\lambda_1 = 1$ and $\lambda_2 = \lambda_3 = 0$. On this vertex one needs $\sigma_1 = 1$, and $\sigma_2 = \sigma_3 = 0$. We have

$$\sigma_1\big|_{\lambda_1=1} = \frac{1}{2}\left(\sigma_1^2\big|_{\lambda_1=1} + \sigma_1^3\big|_{\lambda_1=1} \right).$$

Due to symmetry we know $\sigma_1^2 = \sigma_1^3$ on this vertex. Therefore, we have to let $\sigma_1^2\big|_{\lambda_1=1} = \sigma_1^3\big|_{\lambda_1=1} = 1$. Meanwhile,

$$\sigma_2\big|_{\lambda_1=1} = \frac{1}{2}\big(\sigma_2^2\big|_{\lambda_1=1} + \sigma_2^3\big|_{\lambda_1=1}\big) = 0.$$

This induces us to impose $\sigma_2^2 = \sigma_2^3 = 0$ on this vertex. Next, consider the case on the side where $\lambda_1 = 0$. By Lemma 3.5, $\sigma_1 = 0$. Recalling the consistency constraints (19), we have

$$\sigma_2 - \sigma_3 = \lambda_2 - \lambda_3. \tag{41}$$

Consider any point $\mathbf{P}$ on the side $\lambda_1 = 0$. Then, in (39), the function σ_1^1 takes its value at $\mathbf{P}$ itself, while σ_1^2 is evaluated at the vertex $\lambda_3 = 1$, and σ_1^3 is evaluated at the vertex $\lambda_2 = 1$. Then, on this side, we have

$$\begin{aligned}\sigma_1 &= \frac{1}{2}(\lambda_2+\lambda_3)\sigma_1^1 + \frac{1}{2}(\lambda_1+\lambda_3)\ \sigma_1^2\big|_{\lambda_3=1} + \frac{1}{2}(\lambda_1+\lambda_2)\ \sigma_1^3\big|_{\lambda_2=1}\\ &= \frac{1}{2}\sigma_1^1 + \frac{1}{2}\lambda_3\ \sigma_1^2\big|_{\lambda_3=1} + \frac{1}{2}\lambda_2\ \sigma_1^3\big|_{\lambda_2=1}\\ &= \frac{1}{2}\sigma_1^1 = 0.\end{aligned}$$

This proves that $\sigma_1^1 = 0$ on this side.

The above discussions show that σ_i^i vanishes both at the vertex with $\lambda_i = 1$ and on the side with $\lambda_i = 0$. Also, recall that σ_i^i is constant along straight lines passing through the vertex $\lambda_1 = 1$. Hence it is zero on the whole triangle. By symmetry, we have $\sigma_i^i \equiv 0$, $i = 1,2,3$, on the whole triangle.

□

We now turn to specifying σ_i^j on the sides. On the side where $\lambda_1 = 0$, we also have

$$\begin{aligned}\sigma_2 =& \frac{1}{2}(\lambda_2+\lambda_3)\sigma_2^1 + \frac{1}{2}(\lambda_1+\lambda_3)\ \sigma_2^2\big|_{\lambda_3=1} + \frac{1}{2}(\lambda_1+\lambda_2)\ \sigma_2^3\big|_{\lambda_2=1}\\ =& \frac{1}{2}\sigma_2^1 + \frac{1}{2}\lambda_2\ \sigma_2^3\big|_{\lambda_2=1} \qquad \text{notice } \sigma_2^3 = 1 \text{ on this vertex}\\ =& \frac{1}{2}\sigma_2^1 + \frac{1}{2}\lambda_2,\end{aligned}$$

and

$$\sigma_3 = \frac{1}{2}\sigma_3^1 + \frac{1}{2}\lambda_3.$$

Substracting these two equations yields

$$\sigma_2 - \sigma_3 = \frac{1}{2}(\sigma_2^1 - \sigma_3^1) + \frac{1}{2}(\lambda_2 - \lambda_3).$$

By (41), we have

$$\sigma_2^1 - \lambda_2 = \sigma_3^1 - \lambda_3.$$

Recalling our previous assumption that σ_2^1 and σ_3^1 are independent of λ_1 and F_1, one has to set

$$\begin{aligned}\sigma_2^1 &= \lambda_2 + h\left(\lambda_2, \lambda_3; F_2, F_3\right),\\ \sigma_3^1 &= \lambda_3 + h\left(\lambda_2, \lambda_3; F_2, F_3\right),\end{aligned} \tag{42}$$

where h is a function with symmetry

$$h(x, y; F_x, F_y) = h(y, x; F_y, F_x).$$

The only thing remaining is to specify a particular function h, so that all σ_i^j, $i \neq j$, would be assigned. In choosing the function h, we have some constraints. For example:

(1) On all three vertices, the values of σ_k^j given by (42) are consistent with the discussions above.
(2) The ansatz should cover the equilibrium distribution at the barycenter of the triangle.

With these constraints, our objective is to find an h for which the region where $\hat{I}_B$ is a non-negative integrable function is as large as possible. The requirements for h can be summarized in the following lemma:

Lemma 3.10. *Consider the case when $\lambda_1 = 0$. For consistency with previous constraints on the vertices, the need to contain equilibrium, and to generate a non-negative ansatz for all moments within the region specified by Lemma 3.5, h should satisfy the following:*

(1) $h(\lambda_2, \lambda_3; F_2, F_3) \leq 0$, *within the rectangle* $|F_j| \leq \lambda_j$, $j = 2, 3$.
(2) $-\frac{1}{2}h(\lambda_2, \lambda_3; F_2, F_3) \leq \min\{\lambda_2 - |F_2|, \lambda_3 - |F_3|\}$.
(3) $h(0, 1; 0, F_y) = 0$, $h(1, 0; F_x, 0) = 0$.
(4) $h(\frac{1}{2}, \frac{1}{2}, 0, 0) = -\frac{1}{3}$.
(5) $h(x, y; \pm x, \pm y) = 0$.

Proof. Items 1 and 2 come from requiring $\hat{I}_B$ to be a non-negative distribution for the rectangle region in Lemma 3.5. Recalling that on the side $\lambda_1 = 0$, we have

$$\sigma_j = \lambda_j + \frac{1}{2}h(\lambda_2, \lambda_3; F_2, F_3), \quad j = 2, 3. \tag{43}$$

From Lemma 3.5, a non-negative distribution for (14) in such cases require $|F_j| \leq \sigma_j \leq \lambda_j$, $j = 2, 3$. Hence

$$h(\lambda_2, \lambda_3; F_2, F_3) \leq 0,$$

and

$$-\frac{1}{2}h(\lambda_2, \lambda_3; F_2, F_3) \leq \min\{\lambda_2 - |F_2|, \lambda_3 - |F_3|\}.$$

Item 3 is due to consistency on vertices. For instance, consider the case when $\lambda_2 = 1$, which should correspond to $\sigma_2|_{\lambda_2=1} = 1$, $\sigma_3|_{\lambda_2=1} = 0$. Plugging these into (43) gives item 3.

Item 4 comes from recovering equilibrium. At equilibrium, $\lambda_j = \dfrac{1}{3}$, $F_j = 0$, $j = 1, 2, 3$. Direct calculation gives item 4.

Item 5 also derives from the non-negativity of the ansatz. It is a direct consequence of the discussions in Lemma 3.5. In fact, it will naturally be satisfied if both requirements 1 and 2 are satisfied. However, unlike either, it poses a direct constraint on the value of h at certain points, which, therefore, is particularly useful when trying to propose a formula for h. $\square$

In seeking $h(x, y; F_x, F_y)$, we start with item 5 in Lemma 3.10, which suggests that $h(x, y; F_x, F_y)$ contains the factor

$$q(x, y; F_x, F_y) = \left(x - \frac{F_x^2}{x}\right)\left(y - \frac{F_y^2}{y}\right). \tag{44}$$

Note that as discussed in Lemma 3.5, $\lambda_2 = 0$ would induce $F_2 = 0$, so this construction also guarantees item 3. Also, $q(\lambda_2, \lambda_3; F_2, F_3) \geq 0$ within the rectangle $|F_j| \leq \lambda_j$, $j = 2, 3$. Therefore, the remaining factor, $h(x, y; F_x, F_y)/q(x, y; F_x, F_y)$ is always non-positive within $|F_j| \leq \lambda_j$, $j = 2, 3$. We choose this factor as a constant scaling of

$$r(x, y; F_x, F_y) = -\left(1 - \frac{F_x^2}{x} - \frac{F_y^2}{y}\right), \tag{45}$$

which is always non-positive within the realizability domain. The constant factor is then given as 4/3 based on item 4 in Lemma 3.10. Therefore, the function h is set as

$$h(x, y; F_x, F_y) = \frac{4}{3} q(x, y; F_x, F_y) r(x, y; F_x, F_y). \tag{46}$$

It is clear that it satisfies all items in Lemma 3.10 except for item 2. The precise depiction of the extent to which item 2 is fulfilled is deferred to the investigation of realizability in the next section.

With h given, the whole model is closed. Direct calculation gives us the closing relation of σ_i, $i = 1, 2, 3$, as below:

$$\begin{aligned} \sigma_1 &= \lambda_1 - g(\lambda_1, \lambda_2; F_1, F_2) - g(\lambda_1, \lambda_3; F_1, F_3), \\ \sigma_2 &= \lambda_2 - g(\lambda_2, \lambda_1; F_2, F_1) - g(\lambda_2, \lambda_3, F_2, F_3), \\ \sigma_3 &= \lambda_3 - g(\lambda_3, \lambda_1; F_3, F_1) - g(\lambda_3, \lambda_2; F_3, F_2), \end{aligned} \tag{47}$$

where

$$g(x, y; F_x, F_y) = \frac{2q(x, y; F_x, F_y)(x + y - 1 - r(x, y; F_x, F_y))}{3(x + y)^2}, \tag{48}$$

satisfying $g(x, y; F_x, F_y) = g(y, x; F_y, F_x)$.

With σ_j given as above, we substitute it into (19) to give w_i, $i = 1, 2, 3$, as

$$\begin{aligned} w_1 &= \sigma_1 + 2g(\lambda_2, \lambda_3; F_2, F_3), \\ w_2 &= \sigma_2 + 2g(\lambda_1, \lambda_3; F_1, F_3), \\ w_3 &= \sigma_3 + 2g(\lambda_1, \lambda_2; F_1, F_2). \end{aligned} \tag{49}$$

Then we plug w_i and σ_i into (35) to get γ_i and δ_i. With formula for w_i, γ_i and δ_i, $i = 1, 2, 3$, we now have the complete closed formula for the ansatz $\hat{I}_B$ in (14).

This closes our 3D B_2 model.

3.5. Outline of procedure for computing 3D B_2 closure. In this section, we give a brief summary of the implementation of the 3D B_2 closure. Given the moments E^0, $\mathbf{E}^1$ and $\mathbf{E}^2$, we find the closing relationship E^3_{ijk} through the following procedure.

(1) Compute the eigensystem of the 3×3 matrix $\mathbf{E}^2$, yielding the eigenpairs $(\lambda_j, \mathbf{R}_j)$, $j = 1, 2, 3$.
(2) Compute the projection of $\mathbf{E}^1$ onto $\mathbf{R}_j$. Let $F_j = \mathbf{E}^1 \cdot \mathbf{R}_j$, $j = 1, 2, 3$.
(3) Compute the intermediate variables σ_j by equation (47), with the formula for function g given by equations (48), (44) and (45).
(4) Compute the intermediate variables w_j by equation (49), again with the formula for function g given by equations (48), (44) and (45).
(5) Compute the projection of $\mathbf{E}^3$ into the eigenspace of $\mathbf{E}^2$ by equation (38).

(6) Compute $E^3_{ijk} = \left\langle(\mathbf{\Omega}\cdot\mathbf{R}_l)(\mathbf{\Omega}\cdot\mathbf{R}_m)(\mathbf{\Omega}\cdot\mathbf{R}_n)\hat{I}_B\right\rangle R_{il}R_{jm}R_{kn}$, where R_{jk} is the j-th component of the eigenvector $\mathbf{R}_k$.

4. Model Properties

In this section, we will study the rotational invariance, realizability, and hyperbolicity of the 3D B_2 model proposed.

The proof of rotational invariance is almost straightforward for our model. This is because all the parameters $\mathbf{R}_i$, w_i, γ_i, and δ_i in the ansatz $\hat{I}_B$ are given as functions of known moments E^0, $\mathbf{E}^1$, and $\mathbf{E}^2$. Consequently, the ansatz is rotationally invariant, so we conclude that the moment system produced by $\hat{I}_B$ has rotational invariance. More precisely, we have

Theorem 4.1. *The 3D B_2 model* (15) *is rotationally invariant.*

Proof. Denote the spatial coordinate $\mathbf{x} = (x, y, z)$. In future discussions we sometimes use the notation $\mathbf{x} = (x_1, x_2, x_3)$. For the rotation matrix $\mathbf{T}$, we denote the rotated velocity by $\tilde{\mathbf{\Omega}} = \mathbf{T}\mathbf{\Omega}$, and the rotated spatial coordinate by $\tilde{\mathbf{x}} = \mathbf{T}\mathbf{x}$. We denote $[\tilde{\mathbf{e}}_x, \tilde{\mathbf{e}}_y, \tilde{\mathbf{e}}_z] = [\mathbf{e}_x, \mathbf{e}_y, \mathbf{e}_z]\mathbf{T}^T$. After the rotation, the known moments are denoted by $\tilde{\mathbf{E}}$, and we write the ansatz before and after the rotation with explicit dependence on the known moments by $\hat{I}_B(t, \mathbf{x}, \mathbf{\Omega}; \mathbf{E})$ and $\hat{I}_B(t, \tilde{\mathbf{x}}, \tilde{\mathbf{\Omega}}; \tilde{\mathbf{E}})$. We use $\tilde{E}^0$, $\tilde{\mathbf{E}}^1$, and $\tilde{\mathbf{E}}^2$ to denote the corresponding moments after the rotation, respectively. Let us define $\tilde{\mathbf{v}}$ as

$$
\begin{aligned}
\tilde{\mathbf{v}} = [\quad & 1, \\
& (\mathbf{\Omega}\cdot\tilde{\mathbf{e}}_x), \quad (\mathbf{\Omega}\cdot\tilde{\mathbf{e}}_y), \quad (\mathbf{\Omega}\cdot\tilde{\mathbf{e}}_z), \\
& (\mathbf{\Omega}\cdot\tilde{\mathbf{e}}_x)^2, \quad (\mathbf{\Omega}\cdot\tilde{\mathbf{e}}_x)(\mathbf{\Omega}\cdot\tilde{\mathbf{e}}_y), \quad (\mathbf{\Omega}\cdot\tilde{\mathbf{e}}_x)(\mathbf{\Omega}\cdot\tilde{\mathbf{e}}_z), \\
& \qquad (\mathbf{\Omega}\cdot\tilde{\mathbf{e}}_y)^2, \quad (\mathbf{\Omega}\cdot\tilde{\mathbf{e}}_y)(\mathbf{\Omega}\cdot\tilde{\mathbf{e}}_z) \quad]^T.
\end{aligned}
$$

It is clear there exists a transformation matrix $\mathbb{T}$ which depends only on $\mathbf{T}$ such that

$$\tilde{\mathbf{v}} = \mathbb{T}\mathbf{v},$$

where $\mathbf{v}$ is defined in (3). Thus, the known moments satisfy $\tilde{\mathbf{E}} = \mathbb{T}\mathbf{E}$ and

$$\tilde{E}^0 = E^0, \quad \tilde{\mathbf{E}}^1 = \mathbf{T}\mathbf{E}^1, \quad \tilde{\mathbf{E}}^2 = \mathbf{T}\mathbf{E}^2\mathbf{T}^T.$$

Consequently, the eigenvectors $\tilde{\mathbf{R}}_i$ of $\tilde{\mathbf{E}}^2$ are $\tilde{\mathbf{R}}_i = \mathbf{T}\mathbf{R}_i$, and thus,

$$
\begin{aligned}
\tilde{\mathbf{\Omega}}\cdot\tilde{\mathbf{R}}_i &= \mathbf{\Omega}\cdot\mathbf{R}_i, \\
\tilde{F}_i &= \tilde{\mathbf{E}}^1\cdot\tilde{\mathbf{R}}_i = \mathbf{E}^1\cdot\mathbf{R}_i = F_i.
\end{aligned}
$$

The given closure for w_i, γ_i, and δ_i are functions of the eigenvalues of $\mathbf{E}^2$ and F_i, $i = 1, 2, 3$. Thus, these parameters are exactly the same before and after the rotation. Therefore, the ansatz after the rotation satisfies

$$
\begin{aligned}
\hat{I}_B(t, \tilde{\mathbf{x}}, \tilde{\mathbf{\Omega}}; \mathbb{T}\mathbf{E}) &= \sum_{i=1}^{3} \frac{1}{2\pi} w_i f(\tilde{\mathbf{\Omega}}\cdot\tilde{\mathbf{R}}_i; \gamma_i, \delta_i) \\
&= \sum_{i=1}^{3} \frac{1}{2\pi} w_i f(\mathbf{\Omega}\cdot\mathbf{R}_i; \gamma_i, \delta_i) = \hat{I}_B(t, \mathbf{x}, \mathbf{\Omega}; \mathbf{E}).
\end{aligned}
$$

Meanwhile, the moment system could be written as

$$\left\langle\left(\frac{\partial}{\partial t} + \sum_{j=1}^{3}\Omega_j\frac{\partial}{\partial x_j} - \mathcal{C}\right)\hat{I}_B(t, \mathbf{x}, \mathbf{\Omega}; \mathbf{E}), v(\mathbf{\Omega})\right\rangle = 0.$$

The moment system for the rotated coordinate could be written as

$$\left\langle \left(\frac{\partial}{\partial t} + \sum_{k=1}^{3} \tilde{\Omega}_k \frac{\partial}{\partial \tilde{x}_k} - \mathcal{C} \right) \hat{I}_B(t, \tilde{\mathbf{x}}, \tilde{\mathbf{\Omega}}; \tilde{\mathbf{E}}), v(\tilde{\mathbf{\Omega}}) \right\rangle = 0. \tag{50}$$

Note that

$$\frac{\partial \hat{I}_B}{\partial t}(t, \tilde{\mathbf{x}}, \tilde{\mathbf{\Omega}}; \tilde{\mathbf{E}}) = \frac{\partial \hat{I}_B}{\partial t}(t, \mathbf{x}, \mathbf{\Omega}; \mathbf{E}), \quad \frac{\partial \hat{I}_B}{\partial \tilde{x}_k}(t, \tilde{\mathbf{x}}, \tilde{\mathbf{\Omega}}; \tilde{\mathbf{E}}) = \sum_{j=1}^{3} T_{kj} \frac{\partial \hat{I}_B}{\partial x_j}(t, \mathbf{x}, \mathbf{\Omega}; \mathbf{E}).$$

Also, a typical right hand side of the radiative transfer equations, such as equation (2) satisfies

$$\mathcal{C}(\hat{I}_B(t, \tilde{\mathbf{x}}, \tilde{\mathbf{\Omega}}; \tilde{\mathbf{E}})) = \mathcal{C}(\hat{I}_B(t, \mathbf{x}, \mathbf{\Omega}; \mathbf{E})).$$

In addition, as

$$\sum_{k=1}^{3} T_{kj} \tilde{\Omega}_k = \Omega_j,$$

equation (50) could be re-written as

$$\left\langle \left(\frac{\partial}{\partial t} + \sum_{j=1}^{3} \Omega_j \frac{\partial}{\partial x_j} - \mathcal{C} \right) \hat{I}_B(t, \mathbf{x}, \mathbf{\Omega}; \mathbf{E}), \mathbb{T} v(\mathbf{\Omega}) \right\rangle = 0.$$

As $\mathbb{T}$ is invertible, the above is equivalent to

$$\left\langle \left(\frac{\partial}{\partial t} + \sum_{j=1}^{3} \Omega_j \frac{\partial}{\partial x_j} - \mathcal{C} \right) \hat{I}_B(t, \mathbf{x}, \mathbf{\Omega}; \mathbf{E}), v(\mathbf{\Omega}) \right\rangle = 0,$$

which is the moment system before rotation. Therefore, the moment systems before and after rotation of coordinates are equivalent, which proves the rotational invariance of the model. □

Let us turn to the realizability of our model. First, we point out that the 3D B_2 model provides a non-negative ansatz even for some moments on the boundary of the realizability domain. For example, the moments satisfying $|F_i| = \lambda_i,\ \forall i = 1, 2, 3$, correspond to ansätze of the form

$$\hat{I}_B = \sum_{i=1}^{3} \left[\alpha_i^+ \delta(\mathbf{\Omega} \cdot \mathbf{R}_i - 1) + \alpha_i^- \delta(\mathbf{\Omega} \cdot \mathbf{R}_i + 1) \right].$$

We recall the following results from Lemma 3.6: if λ_i are distinct positive values, then the eight vertices of the rectangular box $|F_j| \le \lambda_j,\ j = 1, 2, 3$, are the only points on the boundary of the realizability domain where a non-negative ansatz for $\hat{I}_B$ may exist. Moreover, the ansatz contains the equilibrium distribution. Moments satisfying $\lambda_i = \dfrac{E^0}{3}$, $i = 1, 2, 3$, and $\mathbf{E}^1 = \mathbf{0}$ reproduce $\hat{I}_B = \dfrac{E^0}{4\pi}$.

Recall that (23) is a sufficient condition for (14) to give a non-negative ansatz. It is equivalent to

$$0 \le \sigma_i \le w_i, \quad \text{and} \quad \sigma_i w_i \ge F_i^2, \quad i = 1, 2, 3. \tag{51}$$

We examine this condition to check the realizability of our model. Define the following discriminant

$$\Delta \triangleq \min \left\{ w_1\sigma_1 - F_1^2, w_2\sigma_2 - F_2^2, w_3\sigma_3 - F_3^2 \right\}. \tag{52}$$

Instantly, we have

Theorem 4.2. *For $|F_j| \le \lambda_j \ne 0$, $j = 1,2,3$, the 3D B_2 model has a non-negative ansatz $\hat{I}_B$ if*

$$3\lambda_i^2 + \lambda_i(\lambda_j + \lambda_k) - \lambda_j\lambda_k > 0, \quad \forall\ i,j,k,\ \text{mutually different}, \tag{53}$$

and

$$\Delta \ge 0.$$

Proof. We first prove $\sigma_1 \le w_1$. Notice that

$$w_1 - \sigma_1 = 2g(\lambda_2, \lambda_3; F_2, F_3) = \frac{4\left(\lambda_2 - \dfrac{F_2^2}{\lambda_2}\right)\left(\lambda_3 - \dfrac{F_3^2}{\lambda_3}\right)\left(\lambda_2 - \dfrac{F_2^2}{\lambda_2} + \lambda_3 - \dfrac{F_3^2}{\lambda_3}\right)}{3(\lambda_2+\lambda_3)^2}.$$

Also, if $|F_j| \le \lambda_j$, we have

$$\lambda_j - \frac{F_j^2}{\lambda_j} \ge 0.$$

Therefore, inside the rectangular box $|F_j| \le \lambda_j$, $j = 1,2,3$, we have $w_1 - \sigma_1 \ge 0$. Similarly, we could prove $\sigma_2 \le w_2$ and $\sigma_3 \le w_3$.

We now discuss the condition for $\sigma_i \ge 0$, $i = 1,2,3$. We begin by examining σ_1. From (47), we see that for fixed λ_i, $i = 1,2,3$, the function σ_1 monotonically increases for any $|F_j|$. Therefore, if $\sigma_1 \ge 0$ holds for $\mathbf{E}^1 = \mathbf{0}$, then it is valid for the whole rectangular box $|F_j| \le \lambda_j$, $j = 1,2,3$. So, the problem becomes seeking $(\lambda_1, \lambda_2, \lambda_3)$ for which $\sigma_1|_{F_1=F_2=F_3=0} \ge 0$ holds. As

$$\sigma_1|_{F_1=F_2=F_3=0} = \frac{\lambda_1(3\lambda_1^2 + \lambda_1\lambda_2 + \lambda_1\lambda_3 - \lambda_2\lambda_3)}{3(\lambda_1+\lambda_2)(\lambda_1+\lambda_3)},$$

the necessary and sufficient condition for $\sigma_1 > 0$ is

$$3\lambda_1^2 + \lambda_1(\lambda_2 + \lambda_3) - \lambda_2\lambda_3 > 0, \tag{54}$$

which completes our proof. □

From the proof of Theorem 4.2 we have the following corollary.

Corollary 4.1. *Let $\mathbf{E}^1 = \mathbf{0}$. If (53) is valid and $\lambda_i \ne 0$, $\forall i = 1,2,3$, the 3D B_2 model has a non-negative ansatz.*

Proof. In the case of $\mathbf{E}^1 = \mathbf{0}$, $\Delta > 0$ is automatically valid under the conditions specified in the corollary. □

Given λ_i and F_i, $i = 1,2,3$, we could use the condition placed on the discriminant Δ in Theorem 4.2 to verify whether a non-negative ansatz exists. For each fixed $(\lambda_1, \lambda_2, \lambda_3)$, we sample for the whole region within the rectangular box $|F_j| \le \lambda_j$, $j = 1,2,3$. It is found that if $\dfrac{\lambda_i}{E^0} \ge \dfrac{1}{7}$, $i = 1,2,3$, then for any (F_1, F_2, F_3) belonging to the region $|F_j| \le \lambda_j$, $j = 1,2,3$, the 3D B_2 model has a non-negative ansatz. Note that the realizability domain for F_j is the ellipsoid given in Lemma 3.4, and the rectangular box $|F_j| \le \lambda_j$, $j = 1,2,3$, is contained within the ellipsoid, with its eight vertices touching the domain boundary. Figure 2 illustrates the region that is found to admit a non-negative ansatz.

Remark 4.1. *By Lemma 3.8, for $\mathbf{E}^1 = \mathbf{0}$, the third-order moments given by the 3D B_2 ansatz is a zero tensor, equal to that given by M_2. For this particular case, even when there is no non-negative ansatz, the closure relation is still realizable.*

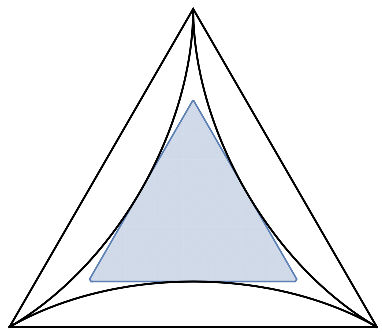

(a) $\left(\frac{\lambda_1}{E^0}, \frac{\lambda_2}{E^0}, \frac{\lambda_3}{E^0}\right)$ are taken as barycentric coordinates within the triangle. The outer triangle is the realizability domain. The curves correspond to the outer boundary of the constraints (53). The blue region gives non-negative ansatz for 3D B_2 model for all $\mathbf{E}^1$ satisfying $|F_j| \le \lambda_j$, $j = 1, 2, 3$.

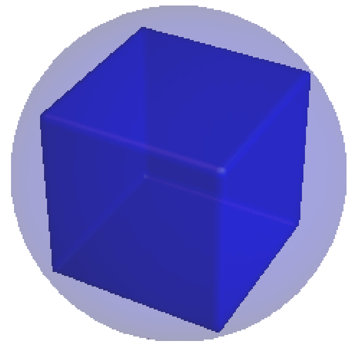

(b) The sphere correspond to the realizability domain of $\mathbf{E}^1$ when $\lambda_1 = \lambda_2 = \lambda_3$.The rectangle within the sphere is the region for $\mathbf{E}^1$ when the 3D B_2 model has a non-negative ansatz.

FIGURE 2. Region which correspond to a non-negative ansatz for 3D B_2 model.

We proceed to study the hyperbolicity of the model. Due to the extreme complexity of the formula, we restrict our discussions to the case that $\mathbf{E}^1 = \mathbf{0}$. We first prove the following facts:

Lemma 4.1. *In the interior of the realizability domain $\mathcal{M}$, if $\mathbf{E}^1 = \mathbf{0}$, we have*

$$w_i > 0, \quad \sigma_i + w_i > 0, \quad i = 1, 2, 3.$$

Proof. Take $i = 1$ for example. First, note

$$g(x, y; 0, 0) = \frac{2q(x, y; 0, 0)(x + y - 1 - r(x, y; 0, 0))}{3(x + y)^2} = \frac{2xy}{3(x + y)}.$$

Therefore,

$$\begin{aligned} w_1 =& \lambda_1 - g(\lambda_1, \lambda_2; 0, 0) - g(\lambda_1, \lambda_3; 0, 0) + 2g(\lambda_2, \lambda_3; 0, 0) \\ =& \frac{1}{3}\left(3\lambda_1 - \frac{2\lambda_1\lambda_2}{\lambda_1 + \lambda_2} - \frac{2\lambda_1\lambda_3}{\lambda_1 + \lambda_3} + \frac{4\lambda_2\lambda_3}{\lambda_2 + \lambda_3}\right) \\ =& \frac{1}{3}\left(\lambda_1 - \frac{2\lambda_1\lambda_2}{\lambda_1 + \lambda_2} + 2\lambda_1 - \frac{2\lambda_1\lambda_3}{\lambda_1 + \lambda_3} + \frac{4\lambda_2\lambda_3}{\lambda_2 + \lambda_3}\right) \\ =& \frac{1}{3}\left(\lambda_1 - \frac{2\lambda_1\lambda_2}{\lambda_1 + \lambda_2} + \frac{2\lambda_1(\lambda_1 + \lambda_3 - \lambda_3)}{\lambda_1 + \lambda_3} + \frac{4\lambda_2\lambda_3}{\lambda_2 + \lambda_3}\right) \\ =& \frac{1}{3}\left(\lambda_1 - \frac{2\lambda_1\lambda_2}{\lambda_1 + \lambda_2} + \frac{2\lambda_1^2}{\lambda_1 + \lambda_3} + \frac{4\lambda_2\lambda_3}{\lambda_2 + \lambda_3}\right). \end{aligned}$$

We need to prove $w_1 \ge 0$ for two cases:

(1) $\lambda_1 \ge \lambda_2$ or $\lambda_1 \ge \lambda_3$. Because w_1 is symmetric with respect to λ_2 and λ_3, we only need to discuss the case $\lambda_1 \ge \lambda_2$.

(2) $\lambda_1 < \lambda_2$ and $\lambda_1 < \lambda_3$. Due to w_1 being symmetric about λ_2 and λ_3, we only need to discuss the case $\lambda_1 < \lambda_2 \leq \lambda_3$.

The proof is as follows:

(1) If $\lambda_1 \geq \lambda_2$, then

$$-\frac{2\lambda_1\lambda_2}{\lambda_1+\lambda_2} \geq -\frac{2\lambda_1\lambda_2}{\lambda_2+\lambda_2} = -\lambda_1,$$

therefore

$$w_1 = \frac{1}{3}\left(\lambda_1 - \frac{2\lambda_1\lambda_2}{\lambda_1+\lambda_2} + \frac{2\lambda_1^2}{\lambda_1+\lambda_3} + \frac{4\lambda_2\lambda_3}{\lambda_2+\lambda_3}\right) \geq \frac{1}{3}\left(\frac{2\lambda_1^2}{\lambda_1+\lambda_3} + \frac{4\lambda_2\lambda_3}{\lambda_2+\lambda_3}\right) > 0.$$

(2) If $\lambda_1 < \lambda_2 \leq \lambda_3$, then

$$-\frac{2\lambda_1\lambda_2}{\lambda_1+\lambda_2} \geq -\frac{2\lambda_1\lambda_2}{\lambda_1+\lambda_1} = -\lambda_2,$$

and

$$\frac{4\lambda_2\lambda_3}{\lambda_2+\lambda_3} \geq \frac{4\lambda_2\lambda_3}{\lambda_3+\lambda_3} = 2\lambda_2.$$

Therefore

$$w_1 = \frac{1}{3}\left(\lambda_1 - \frac{2\lambda_1\lambda_2}{\lambda_1+\lambda_2} + \frac{2\lambda_1^2}{\lambda_1+\lambda_3} + \frac{4\lambda_2\lambda_3}{\lambda_2+\lambda_3}\right) \geq \frac{1}{3}\left(\lambda_1 - \lambda_2 + \frac{2\lambda_1^2}{\lambda_1+\lambda_3} + 2\lambda_2\right) > 0.$$

This proves $w_1 > 0$. Similarly, $w_j > 0$, $j = 2, 3$.

Next, we prove $\sigma_1 + w_1 > 0$. We have

$$\sigma_1 + w_1 = \frac{2}{3}\left(3\lambda_1 - \frac{2\lambda_1\lambda_2}{\lambda_1+\lambda_2} - \frac{2\lambda_1\lambda_3}{\lambda_1+\lambda_3} + \frac{2\lambda_2\lambda_3}{\lambda_2+\lambda_3}\right) = \frac{2}{3}\left(\lambda_1 - \frac{2\lambda_1\lambda_2}{\lambda_1+\lambda_2} + \frac{2\lambda_1^2}{\lambda_1+\lambda_3} + \frac{2\lambda_2\lambda_3}{\lambda_2+\lambda_3}\right).$$

Similar to discussions on w_1, we have

(1) If $\lambda_1 \geq \lambda_2$, then

$$\sigma_1 + w_1 = \frac{2}{3}\left(\lambda_1 - \frac{2\lambda_1\lambda_2}{\lambda_1+\lambda_2} + \frac{2\lambda_1^2}{\lambda_1+\lambda_3} + \frac{2\lambda_2\lambda_3}{\lambda_2+\lambda_3}\right) \geq \frac{2}{3}\left(\frac{2\lambda_1^2}{\lambda_1+\lambda_3} + \frac{2\lambda_2\lambda_3}{\lambda_2+\lambda_3}\right).$$

(2) If $\lambda_1 < \lambda_2 \leq \lambda_3$, then

$$\sigma_1 + w_1 = \frac{2}{3}\left(\lambda_1 - \frac{2\lambda_1\lambda_2}{\lambda_1+\lambda_2} + \frac{2\lambda_1^2}{\lambda_1+\lambda_3} + \frac{2\lambda_2\lambda_3}{\lambda_2+\lambda_3}\right) \geq \frac{2}{3}\left(\lambda_1 - \lambda_2 + \frac{2\lambda_1^2}{\lambda_1+\lambda_3} + \lambda_2\right) > 0.$$

Similarly, $\sigma_i + w_i > 0$, $i = 2, 3$. □

To study hyperbolicity, we start with calculating the Jacobian matrix of the flux $\mathbf{f}_x$, $\mathbf{f}_y$, and $\mathbf{f}_z$. Due to the rotational invariance of the 3D B_2 model, it could be assumed without loss of generality that $\mathbf{E}^2$ is diagonal, $\mathbf{R}_1$ is parallel to the x-axis, $\mathbf{R}_2$ is parallel to the y-axis, and $\mathbf{R}_3$ is parallel to the z-axis, respectively. The most involving part in calculating the Jacobian matrix is the derivatives of third-order moments. We first note that, by Lemma 3.8, fixing $\mathbf{E}^1 = \mathbf{0}$ makes the value of all third-order moments zero, no matter what the values of the other moments are. Therefore,

$$\frac{\partial E^3_{ijk}}{\partial E^0} = 0, \quad \frac{\partial E^3_{ijk}}{\partial E^2_{lm}} = 0, \quad \forall i, j, k, l, m = 1, 2, 3.$$

So we only need to compute $\dfrac{\partial E^3_{ijk}}{\partial E^1_l}$. First, we have

$$\begin{aligned}\frac{\partial E^3_{123}}{\partial E^1_l} &= \frac{\partial \left\langle (\mathbf{\Omega}\cdot\mathbf{R}_i)(\mathbf{\Omega}\cdot\mathbf{R}_j)(\mathbf{\Omega}\cdot\mathbf{R}_k)\hat{I}_B\right\rangle}{\partial E^1_l} R_{i1}R_{j2}R_{k3}\\ &= \frac{\partial \left\langle (\mathbf{\Omega}\cdot\mathbf{R}_1)(\mathbf{\Omega}\cdot\mathbf{R}_2)(\mathbf{\Omega}\cdot\mathbf{R}_3)\hat{I}_B\right\rangle}{\partial E^1_l} = 0.\end{aligned}$$

For the terms $\dfrac{\partial E^3_{iij}}{\partial E^1_k}$, we have

$$\frac{\partial E^3_{iij}}{\partial E^1_k} = \frac{\partial \left\langle (\mathbf{\Omega}\cdot\mathbf{R}_l)(\mathbf{\Omega}\cdot\mathbf{R}_m)(\mathbf{\Omega}\cdot\mathbf{R}_n)\hat{I}_B\right\rangle}{\partial E^1_k} R_{li}R_{mi}R_{nj} = \frac{\partial \left\langle (\mathbf{\Omega}\cdot\mathbf{R}_i)^2(\mathbf{\Omega}\cdot\mathbf{R}_j)\hat{I}_B\right\rangle}{\partial E^1_k}.$$

And by

$$F_i = \mathbf{E}^1\cdot\mathbf{R}_i = E^1_1R_{1i} + E^1_2R_{2i} + E^1_3R_{3i},$$

we get $\dfrac{\partial F_i}{\partial E^1_k} = \delta_{ik}$, which is used below in computing $\dfrac{\partial E^3_{iij}}{\partial E^1_k}$.

If $i = j$ and $k \neq i$,

$$\frac{\partial \left\langle (\mathbf{\Omega}\cdot\mathbf{R}_i)^3\hat{I}_B\right\rangle}{\partial E^1_k} = F_i\frac{\partial}{\partial E^1_k}\left(\frac{\sigma_i^2 + 2F_i^2 - 3w_i\sigma_i}{2F_i^2 - w_i\sigma_i - w_i^2}\right) = 0.$$

And if $i \neq j$ and $k \neq j$,

$$\frac{\partial \left\langle (\mathbf{\Omega}\cdot\mathbf{R}_i)^2(\mathbf{\Omega}\cdot\mathbf{R}_j)\hat{I}_B\right\rangle}{\partial E^1_k} = \frac{F_j}{2}\frac{\partial}{\partial E^1_k}\left(1 - \frac{\sigma_j^2 + 2F_j^2 - 3w_j\sigma_j}{2F_j^2 - w_j\sigma_j - w_j^2}\right) = 0.$$

Therefore, the non-zero entries in the Jacobian matrix can be $\dfrac{\partial E^3_{iij}}{\partial E^1_j}$ only. By rotational invariance of the model, we need only study the Jacobian matrix in the

x-direction, $\dfrac{\partial \mathbf{f}_x}{\partial \mathbf{E}}$, which is

$$\mathbf{J}_x = \begin{pmatrix} 0 & 1 & 0 & 0 & 0 & 0 & 0 & 0 & 0 \\ 0 & 0 & 0 & 0 & 1 & 0 & 0 & 0 & 0 \\ 0 & 0 & 0 & 0 & 0 & 1 & 0 & 0 & 0 \\ 0 & 0 & 0 & 0 & 0 & 0 & 1 & 0 & 0 \\ 0 & \dfrac{\partial E^3_{111}}{\partial E^1_1} & 0 & 0 & 0 & 0 & 0 & 0 & 0 \\ 0 & 0 & \dfrac{\partial E^3_{112}}{\partial E^1_2} & 0 & 0 & 0 & 0 & 0 & 0 \\ 0 & 0 & 0 & \dfrac{\partial E^3_{113}}{\partial E^1_3} & 0 & 0 & 0 & 0 & 0 \\ 0 & \dfrac{\partial E^3_{122}}{\partial E^1_1} & 0 & 0 & 0 & 0 & 0 & 0 & 0 \\ 0 & 0 & 0 & 0 & 0 & 0 & 0 & 0 & 0 \end{pmatrix}. \tag{55}$$

For the non-zero entries in $\mathbf{J}_x$, we have the following bounds:

Lemma 4.2. *In the interior of the realizability domain $\mathcal{M}$, if $\mathbf{E}^1 = \mathbf{0}$, we have*

(1) $0 < \dfrac{\partial E^3_{11k}}{\partial E^1_k} < \dfrac{1}{2}$, *for $k = 2,3$;*

(2) $0 < \dfrac{\partial E^3_{111}}{\partial E^1_1} \le 1$ *if and only if $\sigma_1 > 0$.*

Proof. For the first item, we only need to verify for $k = 2$. By Lemma 3.8, one has

$$\begin{aligned} \frac{\partial E^3_{112}}{\partial E^1_2} &= \frac{\partial \left\langle (\boldsymbol{\Omega}\cdot\mathbf{R}_1)^2(\boldsymbol{\Omega}\cdot\mathbf{R}_2)\hat{I}_B\right\rangle}{\partial E^1_2} \\ &= \frac{1}{2}\left(1 - \frac{\sigma_2^2 + 2F_2^2 - 3w_2\sigma_2}{2F_2^2 - w_2\sigma_2 - w_2^2}\right) \\ &= \frac{1}{2}\frac{(w_2-\sigma_2)^2}{w_2(\sigma_2+w_2)}. \end{aligned}$$

By Lemma 4.1 we have $w_2 > 0$ and $\sigma_2 + w_2 > 0$, thus, $\dfrac{\partial E^3_{112}}{\partial E^1_2} > 0$. In addition, from the proof of Theorem 4.2, we have $\sigma_2 \le w_2$, therefore $\dfrac{\partial E^3_{112}}{\partial E^1_2} < \dfrac{1}{2}$.

For the second item, we have by Lemma 3.8,

$$\begin{aligned} \frac{\partial E^3_{111}}{\partial E^1_1} &= \frac{\partial \left\langle (\boldsymbol{\Omega}\cdot\mathbf{R}_1)^3\hat{I}_B\right\rangle}{\partial E^1_1} = \frac{\sigma_1^2 + 2F_1^2 - 3w_1\sigma_1}{2F_1^2 - w_1\sigma_1 - w_1^2} \\ &= \frac{\sigma_1(3w_1-\sigma_1)}{w_1(\sigma_1+w_1)} = 1 - \frac{(w_1-\sigma_1)^2}{w_1(\sigma_1+w_1)} \le 1, \end{aligned}$$

And $\dfrac{\partial E^3_{111}}{\partial E^1_1} > 0$ is equivalent to $\sigma_1(3w_1 - \sigma_1) > 0$. As $\sigma_1 \le w_1$, we have $3w_1 - \sigma_1 \ge 2w_1 > 0$, implying that $\dfrac{\partial E^3_{111}}{\partial E^1_1} > 0$ is equivalent to $\sigma_1 > 0$. □

We now give the condition for the real diagonalizability of the Jacobian matrix $\mathbf{J}_x$ as follows:

Theorem 4.3. *The Jacobian matrix* $\mathbf{J}_x$ *defined in* (55) *is real diagonalizable if and only if* $\sigma_1 > 0$.

Proof. The characteristic polynomial of $\mathbf{J}_x$ is

$$|\lambda \mathbf{I} - \mathbf{J}_x| = \lambda^3 \left(\lambda^2 - \frac{\partial E^3_{111}}{\partial E^1_1}\right)\left(\lambda^2 - \frac{\partial E^3_{112}}{\partial E^1_2}\right)\left(\lambda^2 - \frac{\partial E^3_{113}}{\partial E^1_3}\right), \tag{56}$$

thus zero is a multiple eigenvalue of $\mathbf{J}_x$. The corresponding eigenvectors are

$$(0,0,0,0,0,0,0,0,1)^T, \quad (0,0,0,0,0,0,0,1,0)^T, \quad (1,0,0,0,0,0,0,0,0)^T.$$

In the case that

$$\frac{\partial E^3_{111}}{\partial E^1_1} \ge 0, \quad \frac{\partial E^3_{112}}{\partial E^1_2} \ge 0, \quad \frac{\partial E^3_{113}}{\partial E^1_3} \ge 0,$$

the corresponding eigenvalues of the matrix are

$$\lambda^\pm_1 = \pm\sqrt{\frac{\partial E^3_{111}}{\partial E^1_1}}, \quad \lambda^\pm_2 = \pm\sqrt{\frac{\partial E^3_{112}}{\partial E^1_2}}, \quad \lambda^\pm_3 = \pm\sqrt{\frac{\partial E^3_{113}}{\partial E^1_3}},$$

and the corresponding eigenvectors are

$$\begin{pmatrix} 1 \\ \lambda^\pm_1 \\ 0 \\ 0 \\ |\lambda^\pm_1|^2 \\ 0 \\ 0 \\ \dfrac{\partial E^3_{122}}{\partial E^1_1} \\ 0 \end{pmatrix}, \quad \begin{pmatrix} 0 \\ 0 \\ -1 \\ 0 \\ 0 \\ \lambda^\pm_2 \\ 0 \\ 0 \\ 0 \end{pmatrix}, \quad \begin{pmatrix} 0 \\ 0 \\ 0 \\ -1 \\ 0 \\ 0 \\ \lambda^\pm_3 \\ 0 \\ 0 \end{pmatrix}.$$

It could be verified directly that if any of the eigenvalues $\lambda^\pm_i$, $i = 1,2,3$, equals zero, the Jacobian matrix is not real diagonalizable. If we have

$$\frac{\partial E^3_{111}}{\partial E^1_1} > 0, \quad \frac{\partial E^3_{112}}{\partial E^1_2} > 0, \quad \frac{\partial E^3_{113}}{\partial E^1_3} > 0, \tag{57}$$

by the linear independence of the eigenvectors, one concludes that the Jacobian matrix is real diagonalizable. Then the proof is finished by Lemma 4.2. □

As a direct consequence of Theorem 4.3, the 3D B_2 model is hyperbolic at equilibrium. This can be proved by the following arguments. Let $\mathbf{R}_j$, $j = 1,2,3$ be the three eigenvectors of $\mathbf{E}^2$. Denote the k-th component of the vector $\mathbf{R}_j$ to be R_{kj}. Define the Jacobian matrix of the 3D B_2 model (15) along $\mathbf{R}_j$, $j = 1,2,3$ to be $\sum_{k=1}^{3} R_{kj}\mathbf{J}_k$. Theorem 4.3 shows that for the cases $\mathbf{E}^1 = \mathbf{0}$, condition (53) is the necessary and sufficient condition for the Jacobian matrix along $\mathbf{R}_j$, $\forall j = 1,2,3$ to

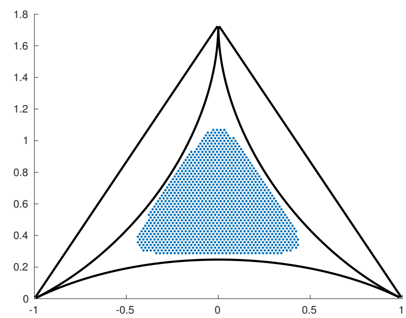

FIGURE 3. Region of hyperbolicity when $\mathbf{E}^1 = \mathbf{0}$. $\left(\frac{\lambda_1}{E^0}, \frac{\lambda_2}{E^0}, \frac{\lambda_3}{E^0}\right)$ are taken as barycentric coordinates within the triangle. The outer triangle is the realizability domain. The curves correspond to the outer boundary of the constraints (53). The 3D B_2 model is found to be hyperbolic within the dotted blue region.

be real diagonalizable. The above result holds because for any given $\mathbf{R}_j$, $j = 1, 2, 3$, we could always rotate the coordinate system, such that $\mathbf{R}_j$ is aligned with the x-axis. Theorem 4.2 gives (54) as the necessary and sufficient condition for $\sigma_1 > 0$, and rotation of coordinates can permute the indices in (54), which results in (53). Notice that at equilibrium, $\mathbf{E}^2$ is a scalar matrix, so any direction is an eigenvector of $\mathbf{E}^2$. Therefore, the 3D B_2 model is hyperbolic at equilibrium.

For given moments, we could always choose a coordinate system such that $\mathbf{E}^2$ is a diagonal matrix. The system is hyperbolic if and only if for an arbitrary $\mathbf{n} \neq \mathbf{0}$, we always have $n_x\mathbf{J}_x + n_y\mathbf{J}_y + n_z\mathbf{J}_z$ to be real diagonalizable. For $\mathbf{E}^1 = \mathbf{0}$, we sample for all possible $(\lambda_1, \lambda_2, \lambda_3)$ and all unit vectors $\mathbf{n}$, to check if the matrix is real diagonalizable. There is a hyperbolicity region around equilibrium for $\mathbf{E}^1 = \mathbf{0}$ as in Figure 3. The hyperbolicity region is a smaller region than that enclosed by (53). However, it does cover a neighborhood of the equilibrium.

Finally, we point out that although the 3D B_2 model is aimed at approximating the M_2 model, there is an interesting difference between them. This difference arises from the fact that the ansatz is assumed to be the form $\hat{I}_B$ in (14), and is independent of choice for the function $f(\mu; \gamma, \delta)$. When the given moments satisfy

$$\exists i \neq j, \text{ such that } \lambda_i = \lambda_j, \text{ and } F_i = F_j = 0, \tag{58}$$

the corresponding ansatz in the M_2 model is an axisymmetric function. This includes the equilibrium distribution. Exactly at the equilibrium, the 3D B_2 ansatz $\hat{I}_B$ is isotropic, and, thus, axisymmetric. However, even in neighbourhoods of the equilibrium, moments corresponding to an axisymmetric ansatz in the M_2 model would usually not reproduce an axisymmetric ansatz for the 3D B_2 model. In other words, for arbitrary $\epsilon > 0$, there exist moments in the set

$$\mathcal{A}_\epsilon = \left\{ (E^0, \mathbf{E}^1, \mathbf{E}^2) \in \mathcal{M} \;\middle|\; \mathbf{E}^1 = \mathbf{0}, \sum_{i=1}^{3} \left| \lambda_i - \frac{E^0}{3} \right|^2 < \epsilon, \text{ and (58) is valid} \right\},$$

for which the 3D B_2 ansatz $\hat{I}_B$ is not axisymmetric; otherwise, the closure relation may lose the necessary regularities. More precisely, we claim:

Theorem 4.4. *There are no functions $w_i(\lambda_1, \lambda_2, \lambda_3; F_1, F_2, F_3)$, $i = 1, 2, 3$, in the 3D B_2 ansatz $\hat{I}_B$ satisfying both items below:*

(1) *w_i, $i = 1, 2, 3$, are differentiable at the equilibrium state.*
(2) *The ansatz $\hat{I}_B$ is axisymmetric for any moments in $\mathcal{A}_\epsilon$.*

Proof. We prove by contradiction. Suppose that (14) is an axisymmetric distribution. Without losing generality we assume the corresponding moments satisfy $\lambda_2 = \lambda_3$, therefore the symmetric axis is aligned to $\mathbf{R}_1$, and $F_2 = F_3 = 0$. To get axisymmetry in (14), the contributions from $w_2 f(\mathbf{\Omega}\cdot\mathbf{R}_2; \gamma_2, \delta_2)$ and $w_3 f(\mathbf{\Omega}\cdot\mathbf{R}_3; \gamma_3, \delta_3)$ have to be either zero or constant functions, hence $\sigma_2 = \dfrac{w_2}{3}$ and $\sigma_3 = \dfrac{w_3}{3}$, giving

$$\sigma_1 + \sigma_2 + \sigma_3 = \lambda_1.$$

Similar relations could be obtained when the symmetric axis is aligned to $\mathbf{R}_2$ or $\mathbf{R}_3$. Consider the case when $\mathbf{E}^1 = \mathbf{0}$. Let

$$\sigma(\lambda_1, \lambda_2, \lambda_3) = \sigma_1(\lambda_1, \lambda_2, \lambda_3; 0, 0, 0) + \sigma_2(\lambda_1, \lambda_2, \lambda_3; 0, 0, 0) + \sigma_3(\lambda_1, \lambda_2, \lambda_3; 0, 0, 0).$$

Based on the above arguments, we have

$$\sigma(\lambda_1, \lambda_2, \lambda_3) = \begin{cases} \lambda_1, & \text{if} \quad \lambda_2 = \lambda_3 = \frac{1}{2}(E^0 - \lambda_1), \\ \lambda_2, & \text{if} \quad \lambda_1 = \lambda_3 = \frac{1}{2}(E^0 - \lambda_2), \\ \lambda_3, & \text{if} \quad \lambda_1 = \lambda_2 = \frac{1}{2}(E^0 - \lambda_3). \end{cases} \tag{59}$$

If all w_i, $i = 1, 2, 3$, are differentiable, then all σ_i, $i = 1, 2, 3$, are differentiable, so $\nabla\sigma$ should be a continuous function for all realizabile moments. Let

$$\mathbf{n}_1 = (1, -\frac{1}{2}, -\frac{1}{2}), \quad \mathbf{n}_2 = (-\frac{1}{2}, 1, -\frac{1}{2}), \quad \mathbf{n}_3 = (-\frac{1}{2}, -\frac{1}{2}, 1),$$

then $\nabla\sigma \cdot (\mathbf{n}_1 + \mathbf{n}_2 + \mathbf{n}_3) = 0$. On the other hand, $\nabla\sigma \cdot \mathbf{n}_1$ is equivalent to taking the derivative of σ along $\lambda_2 = \lambda_3 = \frac{1}{2}(E^0 - \lambda_1)$, and we have similar relationships for $\mathbf{n}_2$ and $\mathbf{n}_3$. So evaluating $\nabla\sigma \cdot \mathbf{n}_j$ at $\lambda_j = \dfrac{E^0}{3}$, $j = 1, 2, 3$ and $\mathbf{E}^1 = \mathbf{0}$ according to (59) gives $\nabla\sigma \cdot (\mathbf{n}_1 + \mathbf{n}_2 + \mathbf{n}_3) = 3$, leading to a contradiction. Therefore the two items can not be satisfied simultaneously. □

Notice that the proof of this lemma does not make use of the specific form of the function f in (14). In fact, it can be seen from the proof that this inconsistency is due to the fact that the ansatz is a linear combination of three axisymmetric distributions. However, although the new model does not reproduce an axisymmetric ansatz for moments corresponding to an axisymmetric ansatz in the M_2 model, in such cases the closure of the new model retain the same structure as the M_2 closure. Without loss of generality consider the case when $\lambda_2 = \lambda_3 = 0$ and $F_2 = F_3 = 0$. From (38), we have

$$\begin{aligned} &\left\langle(\mathbf{\Omega}\cdot\mathbf{R}_1)^2(\mathbf{\Omega}\cdot\mathbf{R}_2)\hat{I}_B\right\rangle = \left\langle(\mathbf{\Omega}\cdot\mathbf{R}_1)^2(\mathbf{\Omega}\cdot\mathbf{R}_3)\hat{I}_B\right\rangle = 0, \\ &\left\langle(\mathbf{\Omega}\cdot\mathbf{R}_1)(\mathbf{\Omega}\cdot\mathbf{R}_2)^2\hat{I}_B\right\rangle = \left\langle(\mathbf{\Omega}\cdot\mathbf{R}_3)(\mathbf{\Omega}\cdot\mathbf{R}_2)^2\hat{I}_B\right\rangle = \frac{1}{2}\left(F_1 - \left\langle(\mathbf{\Omega}\cdot\mathbf{R}_1)^3\right\rangle\right), \end{aligned} \tag{60}$$

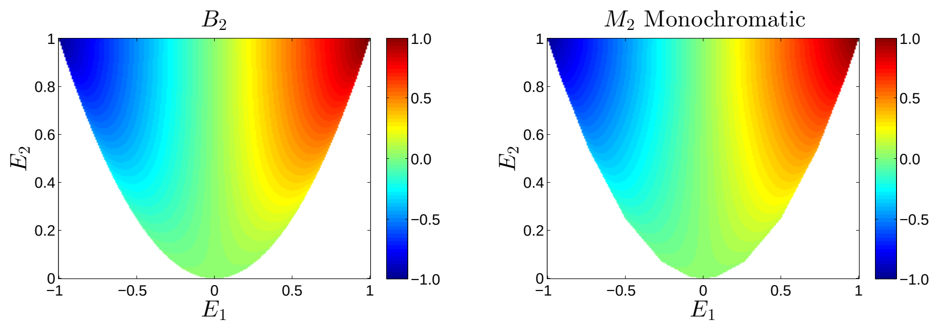

(a) The value of E_3 in slab geometry for normalized realizable moments using the 3D B_2 closure.

(b) The value of E_3 for normalized realizable moments using the maximum entropy closure in slab geometry for the monochromatic case.

FIGURE 4. Comparing the value of the closing moment E_3 for M_2 for the monochromatic case and for the 3D B_2 model in slab geometry.

satisfying the same equalities as that given by an M_2 ansatz with $\mathbf{R}_1$ as the symmetric axis. Define

$$E_1 = \frac{\|\mathbf{E}^1\|}{E^0}, \quad E_2 = \frac{1}{(E^0)^3}(\mathbf{E}^1)^T\mathbf{E}^2\mathbf{E}^1, \quad E_3 = \frac{1}{(E^0)^4}\left\langle\left(\mathbf{\Omega}\cdot\mathbf{E}^1\right)^3\hat{I}\right\rangle.$$

Then E_i, $i = 1,2,3$ would be the scaled first, second and third-order moments for slab geometry cases. We compare the contour of E_3 between the 3D B_2 model and the M_2 model for slab geometry[6] in Figure 4. It is shown in Figure 4 that the 3D B_2 model provides realizable closure which is qualitatively similar to that of M_2 closure for most of realizable moments.

5. Numerical Results

In this section, we study several typical examples to investigate the behaviour of the 3D B_2 moment system. We restrict our numerical simulations to cases where there are only spatial variations in the x and y directions, and the specific intensity is an even function with respect to the z-axis. Hence $E_3^1 = E_{13}^2 = E_{23}^2 = 0$. The variables in the moment system are

$$\mathbf{E} = [E^0, E_1^1, E_2^1, E_{11}^2, E_{12}^2, E_{22}^2]^T.$$

For instance, if we consider the equation for pure scattering,

$$\frac{1}{c}\frac{\partial I}{\partial t} + \mathbf{\Omega}\cdot\nabla I = \sigma_s\left(\frac{1}{4\pi}E^0 - I\right). \tag{61}$$

The moment system becomes

$$\frac{\partial \mathbf{E}}{\partial t} + \frac{\partial \mathbf{f}_x(\mathbf{E})}{\partial x} + \frac{\partial \mathbf{f}_y(\mathbf{E})}{\partial y} = \mathbf{r}(\mathbf{E}), \tag{62}$$

[6]The figure for the slab geometry was reproduced based on the data used to plot the corresponding figure in [3], and the computation was carried out by Dr. Alldredge using his own code during our collaboration therein.

where

$$\begin{aligned}
\mathbf{f}_x &= [E^1_1, E^2_{11}, E^2_{12}, E^3_{111}, E^3_{112}, E^3_{122}]^T,\\
\mathbf{f}_y &= [E^1_2, E^2_{21}, E^2_{22}, E^3_{211}, E^3_{212}, E^3_{222}]^T,\\
\mathbf{r} &= [0, -\sigma_s E^1_1, -\sigma_s E^1_2, \sigma_s(E^0/3 - E^2_{11}), -\sigma_s E^2_{12}, \sigma_s(E^0/3 - E^2_{22})]^T.
\end{aligned}$$

We use the canonical second order finite volume scheme with minmode limiter for linear reconstruction. The FORCE numerical flux is employed. For all simulations the CFL number is taken to be 0.1. In all our simulations, the Cartesian mesh is used with equidistant grids in both x and y directions.

Example 5.1 (Gaussian source problem)**.** *This example is similar to the Gaussian source problem studied in* [11]. *Consider Eq.* (61) *for* $\sigma_s = 1000$ *on an unbounded domain with a computational one* $[-2,2]\times[-2,2]$. *Initially, the specific intensity is taken to be a Gaussian distribution in space and isotropic in direction*

$$I_0(\mathbf{x},\mathbf{\Omega}) = \frac{1}{\sqrt{2\pi\theta}}\exp\left(-\frac{x^2+y^2}{2\theta}\right). \tag{63}$$

We take $\theta = 10^{-2}$ and $c = 1$. The 400×400 mesh grid is used for spatial discretization. In Figure 5, we compare the results of the B_2 model at $ct_{end} = 1.5$ with that of the P_{10} model, and they are in good agreement with each other. Also, it is evident from Figure 5(a), which presents the contour of the solution for E^0 by the B_2 model, that the B_2 model satisfies rotational invariance.

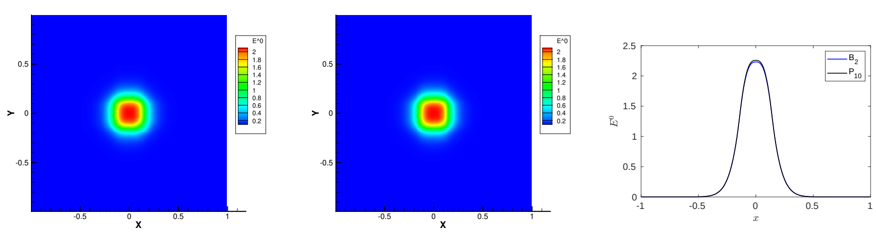

(a) Contour plot of the solution of E^0 of the B_2 model as a function of the spatial coordinate at $ct = 1.5$.

(b) Contour plot of the solution of E^0 by P_{10} as a function of the spatial coordinate at $ct = 1.5$.

(c) Slice in horizontal direction $y = 0$ of the solution of E^0 by B_2 model and P_{10} as a function of x at $ct = 1.5$.

FIGURE 5. Numerical results of the Gaussian source problem.

Example 5.2 (Su-Olson problem)**.** *This example studies the Su-Olson benchmark problem* [25], *where radiation transport is coupled with material energy evolution:*

$$\left\{\begin{aligned}
&\frac{1}{c}\frac{\partial I}{\partial t} + \mathbf{\Omega}\cdot\nabla I = -\sigma_a\left(I - \frac{1}{4\pi}cu_m\right),\\
&\frac{\partial u_m}{\partial t} = \sigma_a\left(E^0 - cu_m\right).
\end{aligned}\right. \tag{64}$$

The absorption coefficient $\sigma_a = 1$ *and the scattering coefficient* $\sigma_s = 0$. *The external source term satisfies*

$$S = \left\{\begin{array}{l} ac, \ \textit{if}\ 0 \le x \le 0.5,\ 0 \le ct \le 10. \\ 0, \ \textit{otherwise}. \end{array}\right.$$

Initially, radiation and material energy are at equilibrium. For our simulations the initial specific intensity of radiation is taken to be an isotropic distribution with energy density 10^{-2}*. The simulation time interval is from* $t_0 = 0$ *to* $ct = 1$*,* 3.16 *and* 10*.*

In our simulation we take $a = c = 1$. The computational domain is taken to be $[-30, 30] \times [-1, 1]$, large enough such that information has not yet propagated to the left or right boundary. We use 2000 cells in the x-direction and 10 cells in the y-direction. The numerical results are presented in Figure 6, where we compare the solution of E^0 and the material energy by the 3D B_2 model and the well-known diffusion approximation with the reference solution at different end time $ct_{end} = 1,\ 3.16,\ 10$. The solution of the diffusion approximation and the semi-analytical reference solution are provided by [25]. We see that the B_2 solution agrees with the benchmark solution values quantitatively better than the diffusion approximation.

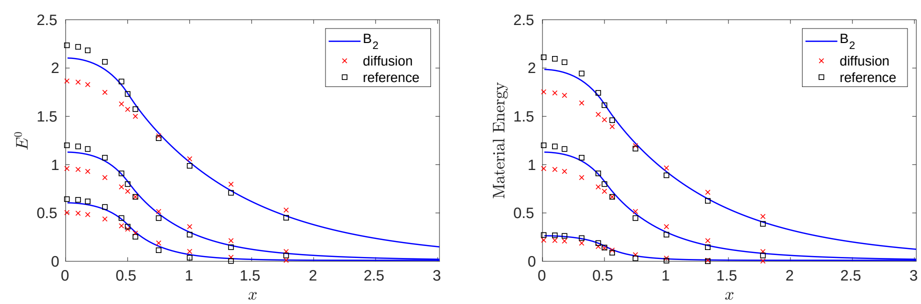

(a) Comparison of the solution of E^0 by the 3D B_2 model and the diffusion approximation as a function of the spatial coordinate x at $ct = 1$, 3.16 and 10 (from down to up).

(b) Comparison of the solution of the material energy by the 3D B_2 model and the diffusion approximation as a function of the spatial coordinate x at $ct = 1$, 3.16 and 10 (from down to up).

FIGURE 6. Numerical results of the Su-Olson benchmark.

Example 5.3 (Radiating disk problem)**.** *The setup of this example is the same as the previous one, except that we take* $\sigma_a = 20$ *and the external source is defined on a disk:*

$$S = \begin{cases} ac, & \text{if } \sqrt{x^2 + y^2} \le 0.5,\ 0 \le ct \le 10. \\ 0, & \text{otherwise.} \end{cases}$$

For our simulation the computation domain is taken to be $[-30, 30] \times [-30, 30]$, and 800×800 cells are used. Figure 7(a) and Figure 7(b) presents the contour plot of E^0 given by the 3D B_2 model and the P_{10} model at $ct_{end} = 10$ and they are consistent with each other. Both models are shown to be rotationally invariant. We compare the results of E^0 by the B_2 model and the P_{10} model at $ct_{end} = 1.5$, 3.75 and 10 in Figure 7(c), and they agree with each other well.

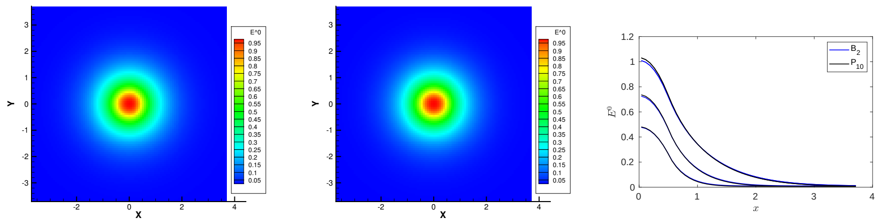

(a) Contour plot of the solution of E^0 of the B_2 model as a function of the spatial coordinate at $ct = 10$.

(b) Contour plot of the solution of E^0 by P_{10} as a function of the spatial coordinate at $ct = 10$.

(c) Slice in horizontal direction $y = 0$ of the solution of E^0 by B_2 model and P_{10} as a function of x at $ct = 1.5$, 3.75 and 10 from down to up.

FIGURE 7. Numerical results of the radiating disk problem.

6. Conclusion Remarks

We proposed a 3D B_2 model that is an extension of the similar model in 1D. We showed, step by step, how the structure of the new model is gradually refined. And we carefully studied those important properties of this new model, including rotational invariance, realizability, and hyperbolicity.

Acknowledgements

The authors appreciate the financial supports provided by the National Natural Science Foundation of China (NSFC) (Grant No. 11421110001 and 11421101) and by the Specialized Research Fund by the State Key Laboratory of Space Weather, Chinese Academy of Sciences.

References

[1] Alldredge, G. W., Hauck, C. D., O'Leary, D. P. and Tits, A. L., Adaptive change of basis in entropy-based moment closures for linear kinetic equations. Journal of Computational Physics, 258:489–508, 2014.

[2] Alldredge, G. W., Hauck, C. D. and Tits, A. L., High-order entropy-based closures for linear transport in slab geometry II: A computational study of the optimization problem. SIAM Journal on Scientific Computing, 34(4):B361–B391, 2012.

[3] Alldredge, G. W., Li, R. and Li, W., Approximating the M_2 method by the extended quadrature method of moments for radiative transfer in slab geometry. Kinetic & Related Models, 9(2):237–249, 2016.

[4] Brunner, T. A. and Holloway, J. P., One-dimensional Riemann solvers and the maximum entropy closure. Journal of Quantitative Spectroscopy and Radiative Transfer, 69(5):543–566, 2001.

[5] Coelho, P. J., Advances in the discrete ordinates and finite volume methods for the solution of radiative heat transfer problems in participating media. Journal of Quantitative Spectroscopy and Radiative Transfer, 145:121–146, 2014.

[6] Curto, R. and Fialkow, L., Recursiveness, positivity and truncated moment problems. Houston J. Math, 17(4):603–635, 1991.

[7] Dubroca, B. and Fuegas, J. L., Étude théorique et numérique d'une hiérarchie de modèles aus moments pour le transfert radiatif. C.R. Acad. Sci. Paris, I. 329:915–920, 1999.

[8] Fleck, J. and Cummings, J., An implicit Monte Carlo scheme for calculating time and frequency dependent nonlinear radiation transport. J. Comput. Phys., 8(3):313–342, 1971.

[9] Frank, M., Dubroca, B. and Klar, A., Partial moment entropy approximation to radiative heat transfer. Journal of Computational Physics, 218(1):1–18, 2006.

[10] Garrett, C. K., Hauck, C. D. and Hill, J., Optimization and large scale computation of an entropy-based moment closure. Journal of Computational Physics, 302:573–590, 2015.
[11] Hauck, C. D., Frank, M. and Olbrant, E., Perturbed, entropy-based closure for radiative transfer. SIAM Journal on Applied Mathematics, 6(3):557–587, 2013.
[12] Hunter, B. and Guo, Z. Comparison of quadrature schemes in DOM for anisotropic scattering radiative transfer analysis. Numerical Heat Transfer, Part B: Fundamentals, 63(6):485–507, 2013.
[13] Johnson, N. L. and Kotz, S., Discrete Distributions: Continuous Univariate Distributions, 2nd Edition. Wiley, 1970.
[14] Junk, M., Maximum entropy for reduced moment problems. Mathematical Models and Methods in Applied Sciences, 10(07):1001–1025, 2000.
[15] Junk, M. and Unterreiter, A., Maximum entropy moment systems and galilean invariance. Continuum Mechanics and Thermodynamics, 14(6):563–576, 2002.
[16] Kershaw, D. S., Flux limiting natures own way. Lawrence Livermore National Laboratory, UCRL-78378, 1976.
[17] Levermore, C. D., Moment closure hierarchies for kinetic theories. Journal of Statistical Physics, 83(5-6):1021–1065, 1996.
[18] Lewis, E. E. and Miller, W. F. Jr., Computational Methods in Neutron Transport. John Wiley and Sons, New York, 1984.
[19] Lucy, L. B., Computing radiative equilibria with Monte Carlo techniques. Astronomy and Astrophysics, 344:282–288, 1999.
[20] McClarren R. G., and Drake, R. P., Anti-diffusive radiation flow in the cooling layer of a radiating shock. Journal of Quantitative Spectroscopy and Radiative Transfer, 111(14):2095–2105, 2010.
[21] Pichard, T., Alldredge, G. W., Brull, S., Dubroca, B. and Frank, M., An approximation of the M_2 closure: Application to radiotherapy dose simulation. Journal of Scientific Computing, 71(1):71–108, 2017.
[22] Pomraning, G. C., The equations of radiation hydrodynamics. Pergamon Press, 1973.
[23] Schneider, F., Kershaw closures for linear transport equations in slab geometry I: Model derivation. Journal of Computational Physics, 322:905 – 919, 2016.
[24] Shohat, J. A. and Tamarkin, J. D., The problem of moments. American Mathematical Soc., 1943.
[25] Su, B. and Olson, G. L., An analytical benchmark for non-equilibrium radiative transfer in an isotropically scattering medium. Annals of Nuclear Energy, 24(13):1035–1055, 1997.
[26] Sun, W., Jiang, S. and Xu, K., An asymptotic preserving implicit unified gas kinetic scheme for frequency-dependent radiative transfer equations. International Journal of Numerical Analysis & Modeling, 15(1-2):134–153, 2018.
[27] Vikas, V., Hauck, C. D., Wang, Z. J., and Fox, R. O., Radiation transport modeling using extended quadrature method of moments. Journal of Computational Physics, 246:221–241, 2013.
[28] Yu, K. B., Recursive updating the eigenvalue decomposition of a covariance matrix. IEEE Transactions on Signal Processing, 39(5):1136–1145, 1991.
[29] Zhou, Z. and Liang, D., A time second-order mass-conserved implicit-explicit domain decomposition scheme for solving the diffusion equations. Advances in Applied Mathematics and Mechanics, 9(4):795–817, 2017.

School of Mathematical Sciences, Peking University, Beijing 100871, China
E-mail: `rli@math.pku.edu.cn`

Applied and Computational Mathematics Division, Beijing Computational Science Research Center, Beijing 100193, China and Department of Mathematics, The Hong Kong University of Science & Technology, Clear Water Bay, Kowloon, Hong Kong.
E-mail: `liweiming@csrc.ac.cn`